



HAL
open science

A review on applications of magnetoelectric composites: from Heterostructural uncooled magnetic sensors, Energy harvesters to Highly efficient power converters

Chung Ming Leung, Jiefang Li, D. Viehland, X. Zhuang

► To cite this version:

Chung Ming Leung, Jiefang Li, D. Viehland, X. Zhuang. A review on applications of magnetoelectric composites: from Heterostructural uncooled magnetic sensors, Energy harvesters to Highly efficient power converters. *Journal of Physics D: Applied Physics*, In press, 10.1088/1361-6463/aac60b . hal-01801976

HAL Id: hal-01801976

<https://hal.science/hal-01801976>

Submitted on 28 May 2018

HAL is a multi-disciplinary open access archive for the deposit and dissemination of scientific research documents, whether they are published or not. The documents may come from teaching and research institutions in France or abroad, or from public or private research centers.

L'archive ouverte pluridisciplinaire **HAL**, est destinée au dépôt et à la diffusion de documents scientifiques de niveau recherche, publiés ou non, émanant des établissements d'enseignement et de recherche français ou étrangers, des laboratoires publics ou privés.

A review on applications of magnetoelectric composites: from Heterostructural uncooled magnetic sensors, Energy harvesters to Highly efficient power converters

Chung Ming Leung*, Jiefang Li, D. Viehland and X. Zhuang*

*Department of Materials Science and Engineering, Virginia Tech, Blacksburg, Virginia
24061, USA*

*Corresponding author E-mail: cmleung@vt.edu; xin2@vt.edu

ABSTRACT

Over the past two decades, magnetoelectric (ME) composites and their devices have been an important topic of research. Potential applications ranging from low power sensing to high power converters have been investigated. This review, first, begins with a summary of multiferroic materials that work at room temperature. Such ME materials are usually in composites, and their ME effect generated as a product property of magnetostrictive and piezoelectric composite layers. After that, mechanisms, working principles, and applications of ME composites from heterostructural uncooled magnetic sensors, energy harvesters to highly efficient power converters will be discussed. First, the development of ME sensors in terms of materials and structures to enhance their sensitivities and to reduce noise level is reviewed and discussed. Second, the structure of ME-based energy harvesters is discussed and summarized. Third, the development ME gyrators is summarized for power applications, including the current/voltage conversion, power efficiency, power density and figures of merit. Results demonstrate that our ME gyrator has the ability to satisfy the needs of power conversion with superior efficiency (>90%), offering potential uses in power electronic applications.

I. Introduction

The term “multiferroic” defines a coexistence of magnetic and electric orderings in a solid. These orderings can polarize as either linear or nonlinear functions in response to an external field: including magnetization (M) and its conjugate magnetic field (H), and polarization (P) and its conjugate electric field (E). The cross-relations between magnetic properties ($M(H)$) and electric properties ($P(E)$) define the magnetoelectric (ME) effect. This cross-coupling results in a change in P due to an applied H (direct ME effect) or a change in M due to an applied E (converse effect). In this case, both the magnetic and electric properties can be mutually controlled. The concept of a ME effect was first suggested by Röntgen in 1888 [1]. He discovered that a dielectric material could be magnetized when placed in a magnetic field. Six years later, Curie suggested that some crystals have intrinsic ME effects [2]. The term magnetoelectric (ME) was first used by Debye in 1926, after studying magnetic and electric field induced changes in dipolar paramagnetic molecules [3]. In 1960, Astrov reported the first observation of magnetic-field-induced electric polarization in antiferromagnetic single crystals of chromium oxide (Cr_2O_3) [4,5]. The ME effect can be subcategorized by its partial differentials into direct and converse effects. The direct ME effect is represented by the ME field coefficient, $\alpha_{\text{ME}} = \frac{dD}{dH}$. It is defined by a change in the dielectric displacement (D) in response to an applied magnetic field (H). The converse effect is represented by $\alpha_{\text{CME}} = \frac{dM}{dV}$. It is defined by a change in the magnetization (M) in response to an applied electric voltage (V).

In the following sections of this article, we will discuss recent progress and present status in the development of bulk ME materials and their applications. We will summarize the results concerning ME composites of macro-laminates, together with background and history, and extend the discussions to recent progress. Detailed reviews of ME materials have previously been published [6–9]. Applications based on ME composites will be presented in more detail in subsequent sections of this review, along with examples of sensors, energy harvesters and power converters that have been recently investigated.

II. Background of ME Materials

Single-phase ME materials have been widely studied in the past decades [10]. A critical limitation for their application is the low transition temperatures of either their ferroelectric or ferromagnetic order parameters, and a weak exchange between them: these prevent their useful applications. To overcome the limitations of single-phase materials, two-phase composites (ferromagnetic/ferroelectric) were first proposed by van Suchtelen in the 1970s [11]. Important advantages of two-phase materials promising practical applications of ME technology were an enhanced ME coefficient that was dramatically higher than single phase materials, as well as increased flexibilities in operational temperature ranges, materials design, manufacturability, and size. Subsequently, strong ME effects have been identified in bulk laminated composites.

In the direct ME effect, a magnetic field applied to the composite produces a mechanical stress/strain in the magnetostrictive phase. This stress/strain results in a mechanical input to the piezoelectric phase which induces a piezoelectric voltage/electric field output proportional to (and of the same frequency) as the input magnetic field. In the converse ME effect, an electric voltage/field applied to the composite results in a mechanical strain in the piezoelectric phase. This strain induces a mechanical stress in the magnetostrictive phase, resulting in a magnetization change. These ME effects can be generically expressed as:

$$\text{Magnetolectric Effect} = \underbrace{\frac{\text{Electric Output/Input}}{\text{Mechanical Input(transfer from/to)}}}_{\substack{\text{Piezoelectric/} \\ \text{Magnetostrictive} \\ \text{Effect}}} \times \underbrace{\frac{\text{Mechanical Output (transfer to/from)}}{\text{Magnetic Input/Output}}}_{\substack{\text{Magnetostrictive/} \\ \text{Piezoelectric} \\ \text{Effect}}}$$

The intermediate strain/stress couplings between the two phases provide several beneficial features to ME composites, such as a stress enhancement of the ME effect at mechanical resonance, which is an oscillatory motion at a specific frequency. In this case, energy is stored as a mechanical form, but not dissipated by the oscillation. A mechanical quality factor Q_{mech} defines the enhancement of the ME coupling at resonance. A standard figure of merit to evaluate the ME effect is the ME coefficient (α_{ME}), which is defined as the value of the output electric voltage across a unit distance (i.e., field) in response to a unit AC magnetic field applied to the ME composite at a given frequency. Its units are V/cm·Oe. A larger value of α_{ME} indicates stronger ME interactions between the two order parameters, *i.e.*, P to H and/or M to E .

In 1974, Boomgarrd *et al.* [12] fabricated a particulate ceramic composite of BaTiO₃-CoFe₂O₄ based on a unidirectional solidification technique. A high value (at that time) of

1
2
3 $\alpha_E=0.13$ V/cm Oe was obtained at room temperature. This value of α_E was $\sim 7\times$ larger than that
4 for single-phase Cr_2O_3 crystals (0.02 V/cm Oe). This is the first example of ME composites
5 having a “product” tensor property, as originally proposed by van Suchtelen [11]. Many types
6 of bulk two-phase ME composites based on product properties have since been fabricated and
7 studied. ME composites can have many different phase interconnectivity structures between
8 ferroelectric and ferromagnetic phases. Research has persisted in bulk composites for 40 years,
9 however, there are several crucial reproducibility and reliability problems that remain
10 unsolvable to date. These are: (1) difficulty in controlling the interconnectivity of the
11 constituent phases; (2) chemical reactions between phases during the sintering process; (3)
12 dielectric breakdown through the low-resistive magnetostrictive phase during poling of the
13 piezoelectric phase; and (4) weak mechanical coupling between phases due to processing-
14 induced mechanical defects such as pores and cracks, amongst other difficulties that have
15 tended to reduce the ME effect and limit its practical applications.

16
17
18
19
20
21
22
23
24
25
26 To overcome these problems of bulk ME composites, laminated composites were first
27 proposed by Ryu *et al.* in 2001 [13]. The laminate configuration was based on a sandwich
28 structure. It combined a thickness-polarized $\text{Pb}(\text{Zr}, \text{Ti})\text{O}_3$ (PZT) piezoelectric ceramic disk,
29 with two radial magnetized Terfenol-D magnetostrictive alloys disks that were bonded by an
30 epoxy adhesive. A large $\alpha_{ME} = 4.68$ V/cm·Oe was found at $f=1$ kHz at room temperature. A
31 year later, the same investigators further enhanced the ME field coefficient to 10.3 V/cm·Oe at
32 an optimal magnetic bias field of 4 kOe by changing the piezoelectric layer from a PZT ceramic
33 to a $\text{Pb}(\text{Mg}_{1/3}\text{Nb}_{2/3})\text{O}_3\text{-PbTiO}_3$ (PMN-PT) piezoelectric crystal [13]. After these initial states,
34 various other composites were reported using piezoelectric and magnetostrictive phases. In the
35 ME laminate composite configuration, the ME coupling is strongly dependent on the
36 magnetostrictive and piezoelectric phase layers, and the interfacial bonding between them. This
37 is because mechanical stress/strain must be transferred between phases with high coupling and
38 low losses. In particular, coupling is strongly dependent on the size and the working mode of
39 both magnetostrictive and piezoelectric phases. The ME coefficient can be enhanced by
40 changing the shape of the ME composite; accordingly, Dong *et al* proposed a sandwich
41 structure in rectangular form and suggested that the best incident direction of a magnetic field
42 was along its in-plane direction [14,15].

43
44
45
46
47
48
49
50
51
52
53
54
55
56
57
58
59
60
Most ME laminated composites have been prepared based on a 2-2 (layer-layer)
connectivity structure and bonded together by an epoxy adhesive or co-firing. Co-fire synthesis
is a good technique to bond all-oxide magnetostrictive and piezoelectric layers. It has an

1
2
3 advantage in cost-effectiveness due to labor-cost reductions. However, the high-temperature
4 co-firing process imparts to the laminated composite several challenges, such as differential
5 shrinkage rates and thermal expansion mismatches. As a consequence, epoxy bonding methods
6 have become the preferred method for fabricated ME laminate composites. They also offer an
7 additional advantage of a low bonding temperature. In the past ten years, the magnetostrictive
8 materials, Terfenol-D ferrites and amorphous metals (Metglas), have been used in ME
9 composites. The maximum effective piezomagnetic coefficient ($d_{\text{eff,m}}$) of Metglas under an
10 optimal magnetic bias is larger than that of Terfenol-D and ferrites. This enhanced effective
11 piezomagnetic coefficient is due to the high permeability of Metglas. The magnetic
12 susceptibility of certain Metglas foils is in order of ~ 10000 , which results in an enhanced
13 effective magneto-mechanical coupling. Due to high $d_{\text{eff,m}}$, and magnetic susceptibility
14 coefficients, and low de-magnetization effects in Metglas, high ME coefficients have been
15 achieved in laminate composites of their foils with piezoelectric layers. A colossal ME
16 coefficient has been reported [16]. This extraordinary high ME coefficient in Metglas/PZT
17 laminated composites has attracted the attention of the research community. It promises
18 applications in magnetic sensors, energy harvesters and power converters [17].
19
20
21
22
23
24
25
26
27
28
29
30

31 Fe-rich Metglas are amorphous metal foils with a giant effective magnetostrictive
32 coefficient. In 2006, Zhai *et al.* [16] reported a Metglas/polyvinylidene-fluoride (PVDF) based
33 ME composite that enhanced the ME coefficient to $7.2\text{V/cm}\cdot\text{Oe}$ at 1 Hz, and up to 310 V/cm at
34 the electromechanical resonance (EMR) frequency under a relatively low dc magnetic bias field
35 of 8 Oe. In the same year, a push-pull design in the piezoelectric layer of Metglas/PZT based
36 ME laminated composites resulted in a further enhancement in the ME coefficient to 22
37 $\text{V/cm}\cdot\text{Oe}$ (at 1 kHz) and $\sim 500\text{ V/cm}\cdot\text{Oe}$ (at resonant frequency) under a magnetic field bias of
38 5 Oe [17]. Later, in 2009, Dong [18] *et al.* showed longitudinal-longitudinal (*L-L*)
39 FeBSiC/PZT/FeBSiC laminates that had a giant ME coefficient of $\sim 750\text{ V/cm}\cdot\text{Oe}$ at EMR due
40 to a high mechanical quality factor in both the Metglas and hard-type PZT phases. More
41 recently, by using Metglas and PMN-PT single crystals, the ME coefficient reached a value of
42 52 V/cm Oe (at 1 kHz) [19] and $>1100\text{ V/cm Oe}$ (at resonant frequency) [20] for push-pull
43 mode ME laminated composites. The ME coefficient in the laminated composites can be further
44 improved by different variables (*i.e.*, size, poling optimization of the piezoelectric layer,
45 annealing of Metglas, mechanical structure, etc.). In 2017, Lasheras *et al.* [21] analyzed the
46 relationship between dimensions and ME coefficient. Three FeCoSiB/PVDF/FeCoSiB ME
47 trilayer laminated composites were fabricated having lengths of 4, 3, 2 cm. It was found that
48
49
50
51
52
53
54
55
56
57
58
59
60

1
2
3 the ME coefficient was increased from 44 V/cm·Oe (2 cm) to 250 V/cm Oe (4 cm) at the EMR.
4 This variation of the ME coefficients with size was attributed to demagnetization effects. In
5 addition to size contribution, Wang *et al.* [22] showed a 1.4× enhancement in the ME coefficient
6 from 31 V/cm·Oe to 42 V/cm·Oe by optimization of the poling temperature and *E*-field ramp
7 rate for PMN-PT. A significant enhancement of the longitudinal piezoelectric d_{33} and k_{33}
8 coefficients was reported when the poling temperature was increased to 120 °C. In 2013,
9 Kirchhof, *et al.* [23] reported a high bending mode ME coefficient of 20000 V/cm Oe (EMR)
10 in FeCoSiB/AlN composites that was measured in a vacuum. Chu *et al.* [24] recently reported
11 longitudinal-transverse (*L-T*) mode ME composites having a 1-D connectivity that consists of
12 PMN-PT and laser-treated amorphous FeBSi Metglas ribbons, which had an ME coefficient of
13 7000 V/cm·Oe (EMR). This large resonance ME coefficient is attributed to the enhancement of
14 the mechanical quality factor (Q_{mech}) of Metglas layers after laser annealing, which is hardened
15 due to crystallization occurring in the Metglas. Thus, the total Q_{mech} of ME composites was
16 enhanced from 200 to 320.
17
18
19
20
21
22
23
24
25
26
27

28 Ferrites are also good magnetostrictive candidate materials in both bulk and laminated ME
29 composites. In 2003, Bichurin *et al.* [25] reported NiFe₂O₄ (NFO)/PZT laminates that had ME
30 coefficient of 23 V/cm Oe (EMR), which was much higher than that previous reported for
31 ferrite/PZT composites. In 2007, an enhanced ME coefficient of 45 V/cm Oe (EMR) was
32 reported in single-crystal-NZFO/PZT composites [26]. In addition, in 2009, Rananaa *et al.* [27]
33 proposed a bulk composite with a high ME coefficient of 3.15 V/Oe cm (non-resonance) that
34 consisted of Ni_{0.93}Co_{0.15}Cu_{0.02}Fe_{1.9}O₄ (NCCFO) and PZT layers. Later, in 2017, Leung *et al.*
35 showed Ni_{0.8}Zn_{0.3}Fe₂O₄ (NZFO) ferrite/PZT/NZFO ferrite laminates that had a much larger ME
36 coefficient of 632 V/cm·Oe (EMR) due to the high mechanical quality factor in both the
37 NZFO/PZT layers [28]. Figure 1 summarizes a list of several ME coefficients that have been
38 reported in the last decade for different configurations and materials, working under non-
39 resonance and resonance conditions.
40
41
42
43
44
45
46
47
48
49
50
51
52
53
54
55
56
57
58
59
60

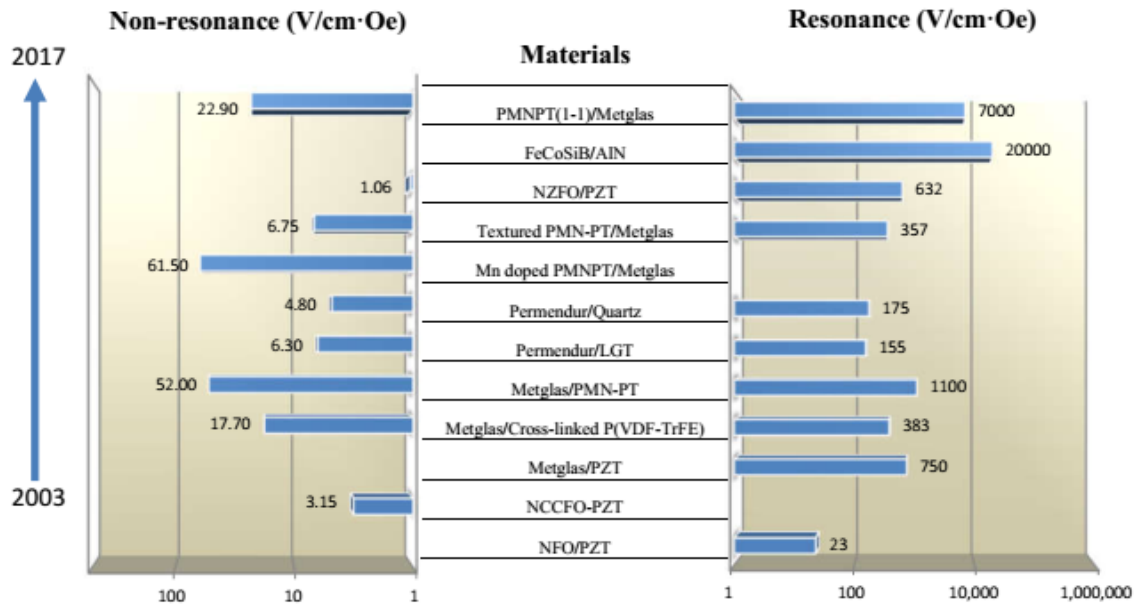


Fig.1. Reported values of non-resonance and resonance ME electric field coefficients for various types of materials [24,23,28-32,19,33,18,27,25], respectively.

Processing and geometry variables have been studied for ME property optimization. For FeSiB Metglas layers, Freeman *et al.* [34] found that annealing in a vacuum environment at 400 °C for 30 min under a magnetic field of 160 mT resulted in an optimal ME coefficient of 6.1 V/cm·Oe in Metglas/PZT composites. Other studies focused on the structural design of ME laminated composites. Enhancements of the ME coefficient have also been found using plane-shaped laminates that combine L - T and shear-shear modes. Xin *et al.* [35] demonstrated a $2\times$ enhancement of the ME coefficient in FeBSiC/PZT laminates, where both ends of the Metglas foils were mechanically clamped by glass to achieve a shear mode configuration.

Semi-ring ME composite structures have been constructed [36] of Ni/PZT/Terfenol-D, as shown in Fig. 2. Since Ni is a negative magnetostrictive material and Terfenol-D is a positive one, the new semi-ring structure exhibited a $1.2\times$ higher ME coefficient (36.1 to 40.5 V/cm Oe) than one of the same configuration that used only positive magnetostrictive materials. Also, a type of ME structure was designed using Terfenol-D, PZT and a nonmagnetic-dielectric trestle which was configured in an A-line type with a shape knuckle joint assembly [37]. This micro-trestle had a maximum ME coefficient $\sim 2\times$ higher than that for conventional laminated ones.

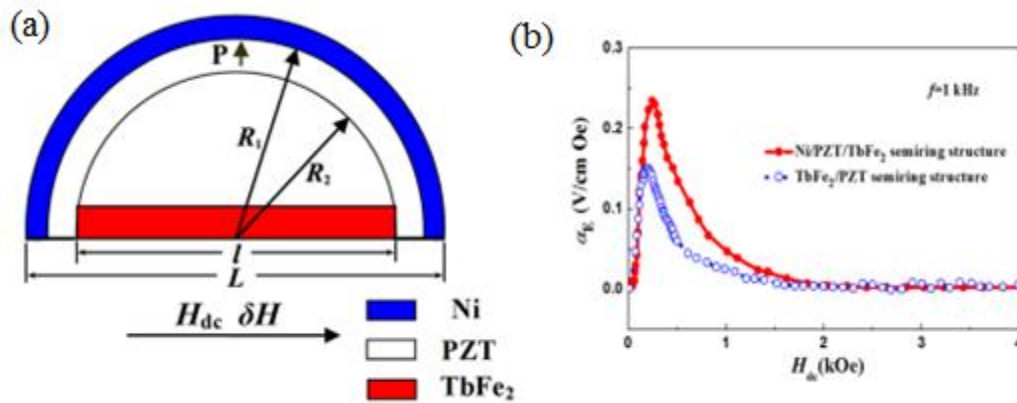


Fig. 2. (a) Schematic geometry arrangement of the Ni/PZT/TbFe₂ semiring structure. (b) Bias magnetic field H_{dc} dependence of ME voltage coefficient α_E at $f = 1$ kHz [36]. Reproduced from *Journal of Applied Physics*, 119, 034102 (2016), with the permission of AIP Publishing.

Using interdigital electrodes, L - L multiple-push pull configurations have been introduced into ME composites. Magnetostrictive FeBSiC alloy ribbons laminated with piezoelectric PZT fibers exhibited a strong resonant ME voltage coefficient of 750 V/cm-Oe (EMR), as shown in Figs. 3 and 4 [18]. The strong enhancement of the ME coefficient can be attributed to the high mechanical quality factor Q_m of the Metglas ribbon and hard-type PZT ceramic fiber.

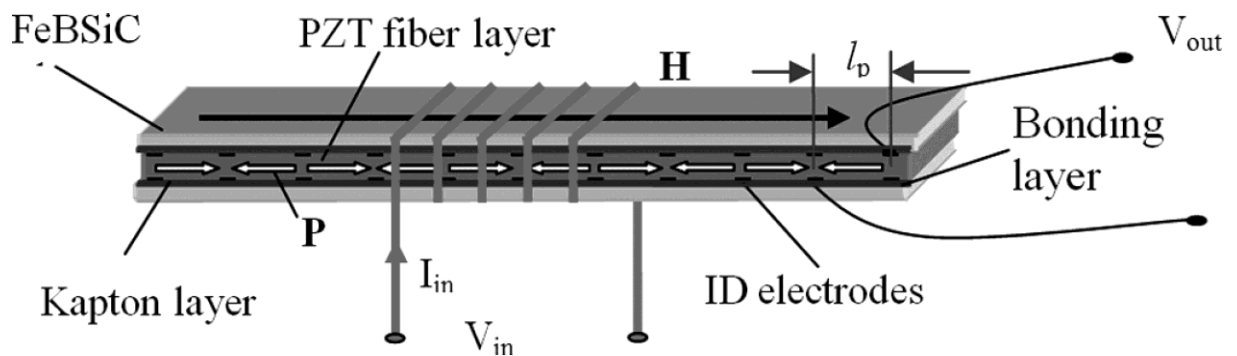


Fig. 3. Magnetoelastic transformer with a 5-layer laminate configuration (2-layer Metglas/1-layer PZT-fiber/2-layer Metglas). The size of the laminate as 100 mm in length, 12 mm in width, and 0.36 mm in thickness [18]. Reproduced from *IEEE Transactions on Ultrasonics, Ferroelectrics, and Frequency Control*, 56, 1124–7 (2009), with the permission of IEEE.

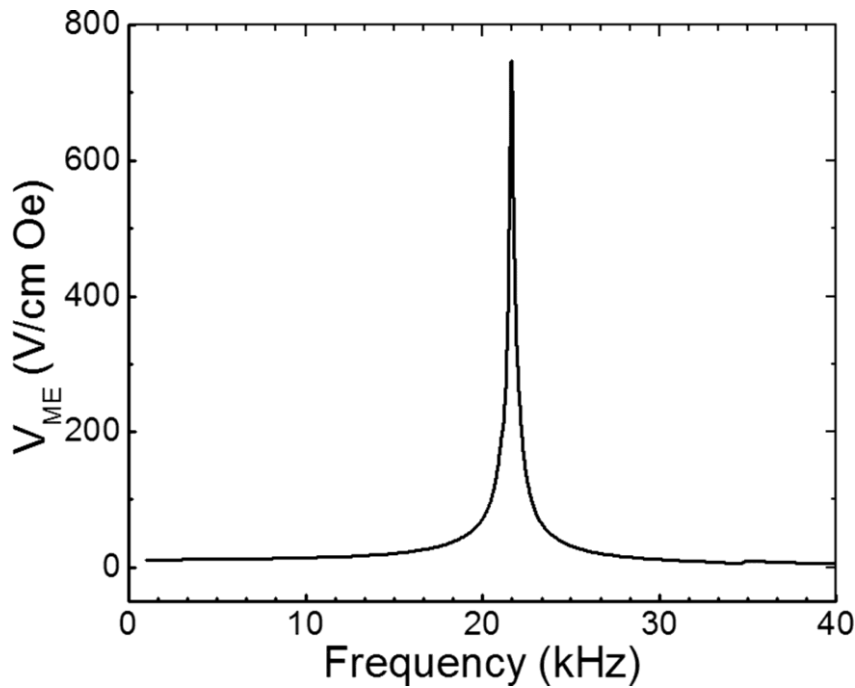


Fig. 4. Magnetolectric voltage coefficient as a function of magnetic field frequency at $H_{dc}=5$ Oe [18]. Reproduced from *IEEE Transactions on Ultrasonics, Ferroelectrics, and Frequency Control*, 56, 1124–7 (2009), with the permission of IEEE.

III. Applications of ME composites

There are several characteristic properties of ME composites that are potentially enabling for applications. The first is a characteristic curve for the ME coefficient as a function of magnetic bias [15]. High magnetically induced strains exist in some soft magnetostrictive materials. A magnetic bias is required to align the magnetization vector along the easy direction to maximize the induced strain. Second, the ME coefficient at the mechanical resonant frequencies can be order(s) of magnitude higher than that at sub-resonant ones. Third, the power loss (or dissipation) in ME composites influences the ME coupling, having an obvious significant effect on the efficiency. Last, ME composites have a tunability feature that results from the shift of the resonant frequency, impedance and output voltage characteristics with bias. These four characteristic features enable potential applications of ME composites in **memory devices, gyrators, magnetic sensors, filters, and resonators.**

Memory devices (Fig. 5) with magnetic/electric write and read have been an important developing focus of ME materials that has attracted the attention of investigators [38]. A memory device based on ME composites could enable low cost and effective write/read speeds at low power consumption. However, a full 180° switching of the magnetization may be

difficult to achieve by strain mediated coupling [39]. *The ability of cross-controlling magnetic and electric polarization may be a key for such switching for this application.*

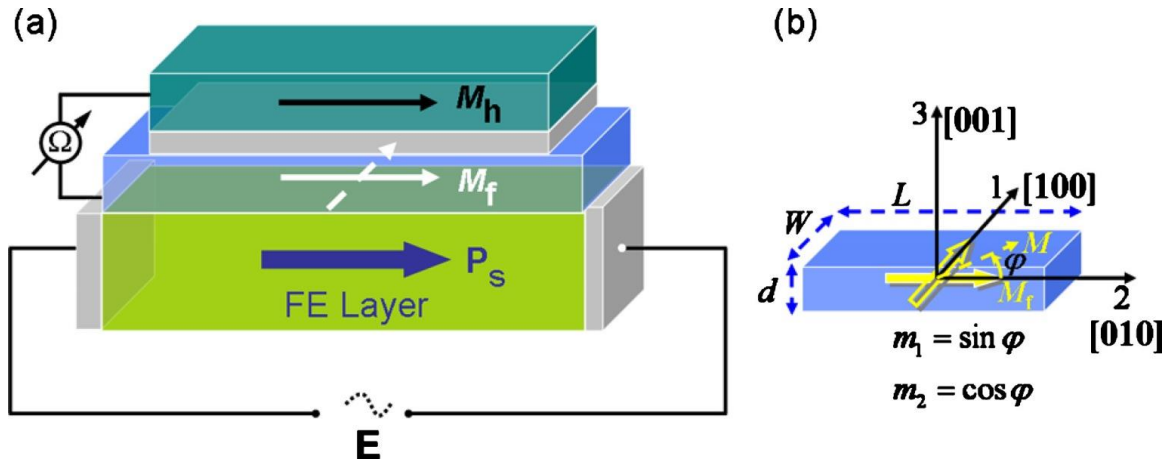


Fig. 5. (a) Schematic diagram of a SME-RAM element. M_h and M_f show the initial magnetization orientations in the upper hard layer and the bottom free layer of a MTJ unit, respectively. A transverse electric field E is applied to the FE layer with a spontaneous polarization P_s to generate a 90° in-plane magnetization switching. (b) the 90° in-plane magnetization switching process in the free layer with its length (L), width (W), and thickness (d) directions along the three principle crystal axes, i.e., the $[010]$, $[100]$, and $[001]$, respectively [38]. Reproduced from *Journal of Applied Physics*, 107, 093912 (2010), with the permission of AIP Publishing.

ME composites with a coil carrying current have a gyration effect, which converts current into a voltage. The **ME gyrotor** (Fig. 6) is a two-port four-wire device [40,41]. Calculations of the impedance parameters of this device have shown that an ideal gyrotor element can be achieved when the square of the ME susceptibility is equal to the product of the permeability and permittivity in the ME composite (*i.e.* $\alpha_{me}^2 = \mu\epsilon$) [41]. The current-to-voltage conversion, or trans-impedance, presents itself as a gyration coefficient. The ME coupling at the resonant frequency is a means to approach an ideal ME gyrotor since power conversion is only appreciably enhanced at resonance: in this case, the equivalence of $\alpha_{me}^2 = \mu\epsilon$ is approximately satisfied. *A key feature of gyrotors is the enhanced ME coupling at the mechanical resonant frequency.*

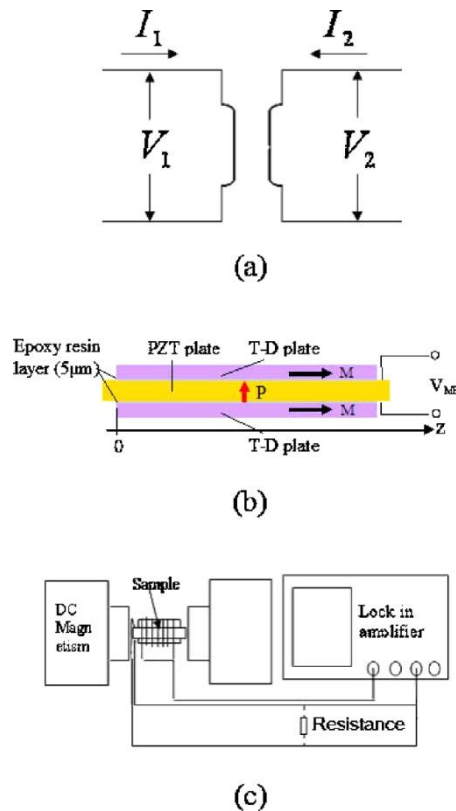


Fig. 6. (a) Gyrator equivalent circuit; (b) illustration of longitudinal-transverse or L - T mode of a magnetoelastic laminate composite consisting of longitudinally poled $\text{Pb}(\text{Zr}_x, \text{Ti}_{1-x})\text{O}_3$ layer sandwiched between two longitudinally magnetized Terfenol-D layers, epoxied together with a thin insulating resin layer; and (c) schematic illustrating the experiment setup [41]. Reproduced from *Journal of Applied Physics*, 100, 124509 (2006), with the permission of AIP Publishing.

Magnetic sensors based on ME composites offer a new generation of passive and active magnetic sensors [19,42–44], as summarized in Fig.7. Noise sources can be either extrinsic or intrinsic. The former is due to unwanted fluctuations that are incident on the ME sensor, *i.e.* magnetic and vibration fluctuations; however, the latter results from the internal power losses via a dissipative term (such as dielectric loss in piezo-phase). ME sensors have several characteristics which are the magnetic transfer function, the noise level and the equivalent magnetic noise (EMN) [45]. The transfer function is the sensing capacity, the noise level is the reliability of the detection and the EMN is the resolution of the sensors. The EMN is calculated by the noise spectral density over the transfer function. A lower level of EMN offers a better sensor sensitivity for measuring the strength of an unknown magnetic field. In addition to the ME coefficient that can enhance the transfer function, *the fluctuation-dissipation term is also a key factor for ME sensors.*

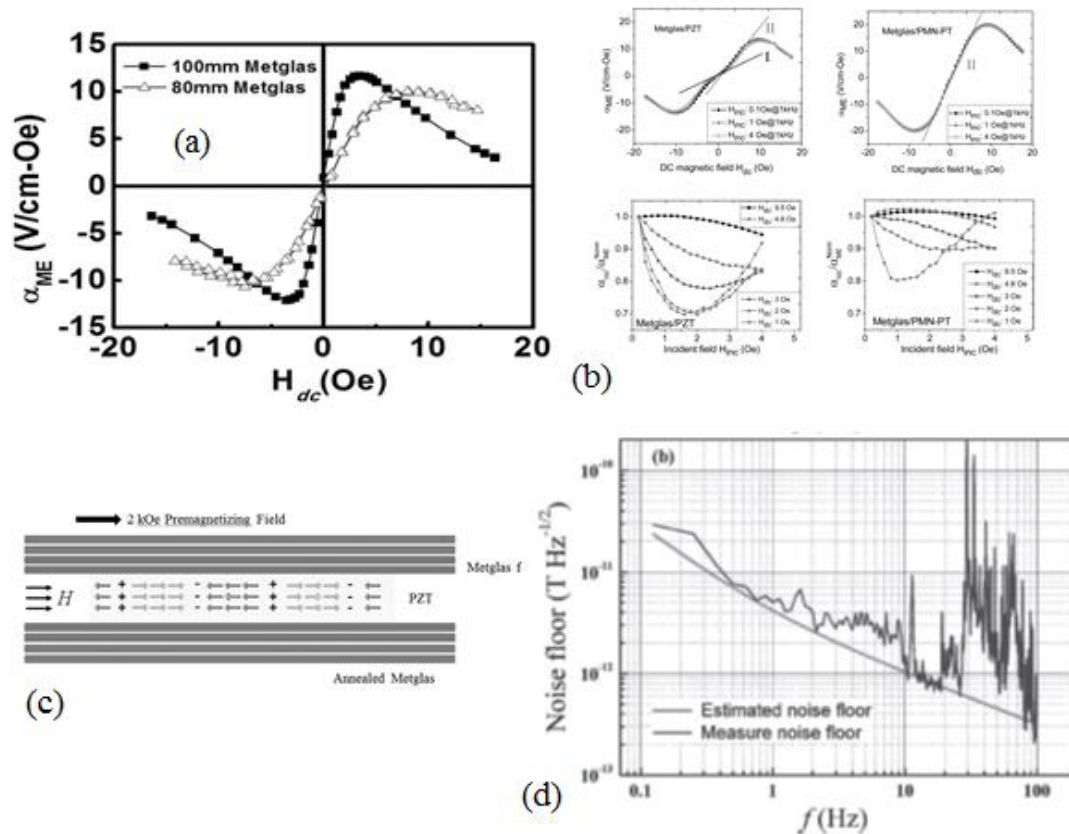


Fig. 7. Linear (a) and nonlinear (b) ME coefficients [42,43], (c) ME sensor in LL multiple push-pull configurations [44] and (d) equivalent magnetic noise spectral density [19]. Reproduced from *Applied Physics Letters*, 99, 153502 (2011), *Journal of Applied Physics*, 110 114510 (2011), *Applied Physics Letter*, 102, 082404, and *Advanced Materials*, 23, 153502 (2011), with the permission of AIP Publishing and Wiley-VCH.

The narrow bandwidth of ME laminate resonators (Fig. 8-9) enables their application as **ME tunable filters/resonators** [46–48]. This is because the resonant frequency can be tuned by applying a magnetic or electric bias field. The signal/power is transmitted over an allowed bandwidth that is determined by the external field strength. Tunable filters/resonators have a certain relation with ME sensors, since the tunability of the resonant frequency can be expressed as a function of the magnetic field strength. Such ME filters/resonators are based on ferrite-piezoelectric composites. Other features of the ferrites that allow the filter/resonator to work at ultrahigh frequencies are *the tunability of the resonant frequency, impedance and ME coefficient are key factors for tunable filters/resonators.*

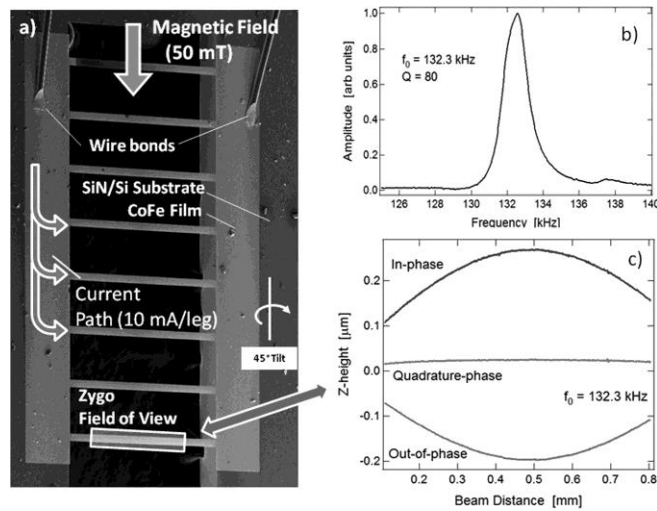


Fig. 8. SEM image of selected beam array showing $40\ \mu\text{m} \times 1\ \text{mm}$ beam set at 45° tilt; (b) Zygo beam resonance spectrum and (c) surface plot and lines can evaluation at named phase angles under Lorentz force excitation [46]. Reproduced from *Applied Physics Letters*, 104, 072408 (2014), with the permission of AIP Publishing.

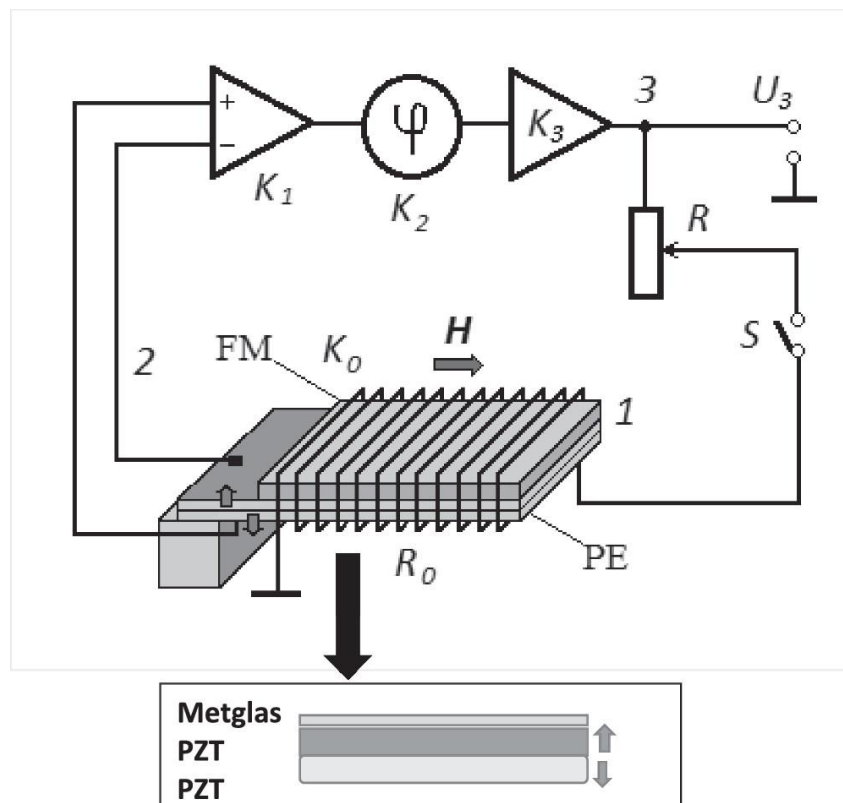


Fig. 9. Block-diagram of the signal generator with a magnetoelastic (ME) composite resonator (1) in the feedback loop (2). The composite is an epoxy bonded layered structure with a piezoelectric (PE) PZT bimorph and a ferromagnetic (FM) Metglas layer. Amplifiers and an RC-phase shifter are also shown. The inset shows the cross section of the composite with PZT bimorph and Metglas layer [48]. Reproduced from *Applied Physics Letters*, 108, 213502 (2016), with the permission of AIP Publishing.

1
2
3 Both ME sensors and gyrators are electronics devices: the former transfers magnetic
4 field/flux into electric signals, and the latter converts the current to a voltage based on trans-
5 impedance. The ME sensor can thus serve as a micro-power convertor at sub-resonant/resonant
6 frequencies. When the magnetic power conversion is high, ME composite can detect a magnetic
7 field with high sensitivity. ME gyrators can also be high-power converters working near their
8 mechanical resonant frequency. When the power conversion is close to unity, a coil-ME
9 structure can be considered as an ideal gyrator.
10
11
12
13
14
15
16
17

18 **Heterostructural uncooled magnetic sensors**

20
21 Magnetic sensors that operate at room temperature with ultrahigh sensitivity have
22 enabling applications for penetration imaging, and tracking and/or communications. Technical
23 goals of ME sensors were to demonstrate a high sensitivity [49]. Target sensitivities from
24 $1\text{fT}/\sqrt{\text{Hz}}$ to $1\text{pT}/\sqrt{\text{Hz}}$ at 1 Hz have been sought. To approach this detection level, the noise
25 source in ME sensors should be reduced, while amplifying the ME gain coefficients by an order
26 of magnitude. Magnetic and piezoelectric materials with high conversion factors are desired by
27 which to fabricate composites of high ME coefficients.
28
29
30
31
32

33 Our team has previously developed ME composites consisting of laminate layers to
34 convert magnetic energy to electric energy, by using symmetric and asymmetric bending mode
35 ME composites [50,52]. A 2-1 connectivity configuration consisting of 1-D piezo-fibers and 2-
36 D FeBSiC Metglas has been reported to have a high ME coefficient of $22\text{ V/cm}\cdot\text{Oe}$ (sub-
37 resonance) and $1000\text{ V/cm}\cdot\text{Oe}$ (EMR). This enhancement was attributed to the colossal
38 effective magnetostrictive coefficient in FeBSiC and the use of piezoelectric materials with
39 high $d_{33,p}$ values in a longitudinal-longitudinal ($L-L$) configuration [51], as shown in Fig. 3. This
40 promised an unleashing of the potential of magnetoelectricity in laminate composites. In
41 addition to the ME coefficient, the loss factor in the piezoelectric constituent phase is an
42 important parameter by which to improve the detection capability. Magnetic sensors based on
43 Metglas and PMN-PT single crystals laminates have shown an extremely low equivalent noise
44 spectral density of $<10\text{ pT}/\sqrt{\text{Hz}}$ at 1 Hz [19,54]. With low power consumption and relatively
45 small size, ME magnetic sensors have been considered as an alternative sensing technology
46 with great potential to displace many existing magnetic sensors technologies. Enhancement of
47 ME coefficients at the EMR pushes the noise floor of ME sensors below $1\text{pT}/\sqrt{\text{Hz}}$ near the
48 resonant frequency [53]. In addition, ME composites can harvest electromagnetic energy, when
49
50
51
52
53
54
55
56
57
58
59
60

excited at its fundamental resonance. The associated amplifier can be charged by harvesting energy, which can enable self-powered ME sensors capable of long-term development [54].

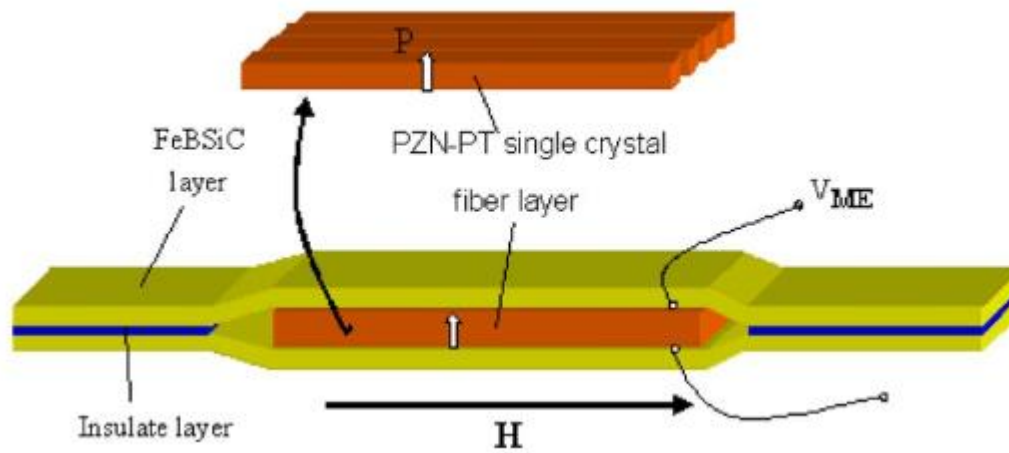


Fig. 10. Structure of FeBSiC/PZNPT-fiber laminate [51]. Reproduced from *Applied Physics Letters*, 91, 022915 (2007), with the permission of AIP Publishing.

The measurement of magnetic sensors with high sensitivity requires a measurement system with lower environmental noise sources. As such, the GREYC-CNRS research group has introduced a method for characterizing ME sensors at low frequency in a 6-layer magnetic shielded room, which has a noise level lower than SQUID sensitivity [45]. Using this measurement system, the noise contributions from several noise sources in both ME sensors and their conditioning detection circuits were studied and analyzed. The results identified that the intrinsic factor that may limit the ME sensor performance is the dielectric loss in the piezoelectric phase. This has been verified by both calculated and measured noise spectral densities. Frequency conversion techniques that shift the low-frequency signals to much higher ones near a carrier signal allows avoiding/reducing the dominant noise at low frequencies. The Army Research Lab (Adelphi, MD) has contributed to this technique by using flux concentrators that have single-support or double clamped ME films of Galfenol on PZT [55]. GREYC realized a noise level of $30\text{-}40\text{pT}/\sqrt{\text{Hz}}$ using Metglas/piezo-fiber ME composites having an excitation carrier at the resonant frequency [56]. Self-biased and symmetric L-T mode ME sensors have been developed by Oakland University [57]. Self-biased sensors operate without magnetic bias, as shown in Fig. 11. The effect is due to a gradient magnetostriction between the two different magnetic phases: this provides sensitivities below $100\text{pT}/\sqrt{\text{Hz}}$ at 1 Hz. Measurements of sensors with different stacking configurations of piezoelectric PZT layers verified a volume scale effect for ME sensors [58]. One dimensional ME composites offer the possibility to overcome the magnetic demagnetization effect. Northeastern University

developed a quasi-one dimension ME sensor consisting of a FeNi/PZT composite, which had a ME coefficient of 1.65V/cm-Oe under zero magnetic bias [59].

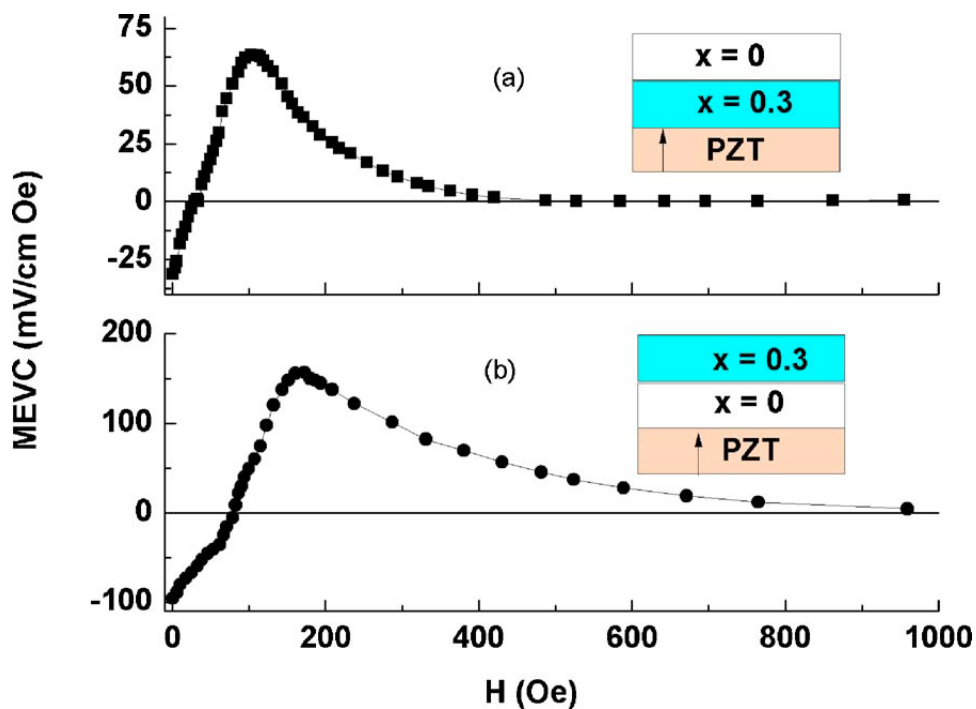


Fig. 11. Bias field dependence of MEVC in bilayers with equal volume of PZT and graded NZFO for (a) negative grading of q and (b) positive grading of q in the ferrite layer [57]. Reproduced from *Applied Physics Letters*, 96, 192502 (2010), with the permission of AIP Publishing.

Structure and geometry optimizations of ME composites have been investigated to enhance the ME sensitivity. This includes a volume scale effect and the optimal thickness ratio for various material combinations, in addition to the bonding in the intermediate layer(s). The ME effect was reported to be increased by means of an optimal mechanical coupling between the magnetostrictive and piezoelectric layers [60]. A specific thickness ratio between magnetic and piezoelectric phases was observed to maximize the ME coefficient. This ratio depended on the coefficients in the ME composite, such as the compliance module of both the magnetic and piezoelectric phases. Strong ME effects were reported for nickel-ferrite/PZT composites. The field sensing ability is related to the field coupling onto the magnetic phase. Thus, the magnetic field conversion for the volume effect needs to be considered for practical applications. The volume effect of the piezoelectric phase has been investigated as well. This includes stacked layers with several ME composites to increase the volume of the piezoelectric phase. An increased volume was identified to result in a lower equivalent magnetic noise level. This is due to the fact that the transfer function increases with increasing volume, but the noise increases as the root of the volume. An improved bonding condition results in a significant

1
2
3 increase in the ME coefficient and a reduction in the equivalent magnetic noise floor.
4 Optimization of the epoxy thickness increases the coupling between the magnetostrictive and
5 piezoelectric layers [61,62]. Thus, a vacuum-bag curing technique was introduced in the ME
6 sensor fabrication [61]. It has been reported that the ME coefficient is dependent on the
7 thickness and Young's modulus of the bonding materials [63]. The ME coefficients decreased
8 as the bonding layer thickness is increased, whereas Young's modulus was decreased.
9

10
11
12
13
14
15
16
17
18
19
20
21
22
23
24
25
26
27
28
29
30
31
32
33
34
35
36
37
38
39
40
41
42
43
44
45
46
47
48
49
50
51
52
53
54
55
56
57
58
59
60

Thin film ME resonators have been studied as magnetic field vector sensors. Sputtered Fe based alloys (TbFe, FeCo) on PZT were investigated, which enhanced the magnetostrictive coefficient above that of Terfenol-D [64]. Interdigital electrodes have been deposited onto the structure of the ME thin films, which was reported to significantly improve the ME coefficient [65]. Recently, FeCoSiB/AlN thin film showed a ME coefficient as large as 6900 V/cm Oe at the bending made mechanical resonant frequency, along with a limit of detection of 1 pT/ $\sqrt{\text{Hz}}$ [66]. The volume effect of ME composite is an important parameter limiting the detection performance of magnetic sensors. The limit of detection of inverse bilayer magneto piezoelectric thin films has been measured to reach 400 fT/ $\sqrt{\text{Hz}}$ at their mechanical resonance, accompanied by a ME coefficient as high as 5000 V/cm Oe [67]. When performed out-of-resonance, detection by thin film sensors falls behind the bulk ones. A suggested solution to enhance the detection ability is the realization of partially released symmetrical thin film composite sensors that would perform a longitudinal expansion of the sensor, rather than a bending mode.

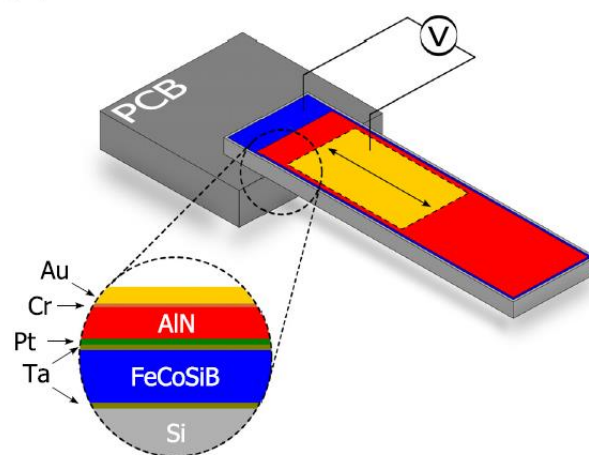


Fig. 12. Schematic illustration of thin film sensor [67]. Reproduced from *Applied Physics Letters*, 109, 022901 (2016), with the permission of AIP Publishing.

The piezoelectric phase in ME composites serves to convert a strain transmitted from the magnetostrictive phase into a voltage/charge output. Because the piezoelectric phase is also

sensitive to vibration fluctuations, ME sensors have limitations in mechanically noisy environments [68]. Various vibration canceling methods have been studied to improve the sensing ability for real-world applications. These methods were based on built-in structures that separate magnetic and vibration induced signals generated by different modes, or by use of adaptive calculations to subtract the vibration noise using a reference vibration/acoustic sensor. Another approach to avoid the influence of vibrations is based on modulation/frequency conversion techniques [69,70]. A low-frequency signal modulates a carrier which is excited in the vicinity of the mechanical resonant frequency, where both the intrinsic noise and external fluctuations are weaker than the one at low frequencies. After a classical demodulation process, the low-frequency signals can be recovered from the sideband signals near the carrier. This working mode also enables quasi-DC field detection capacities for ME composites [71–73]. Materials and structures that optimize the ME sensitivity based on nonlinearity have also been investigated [74–76].

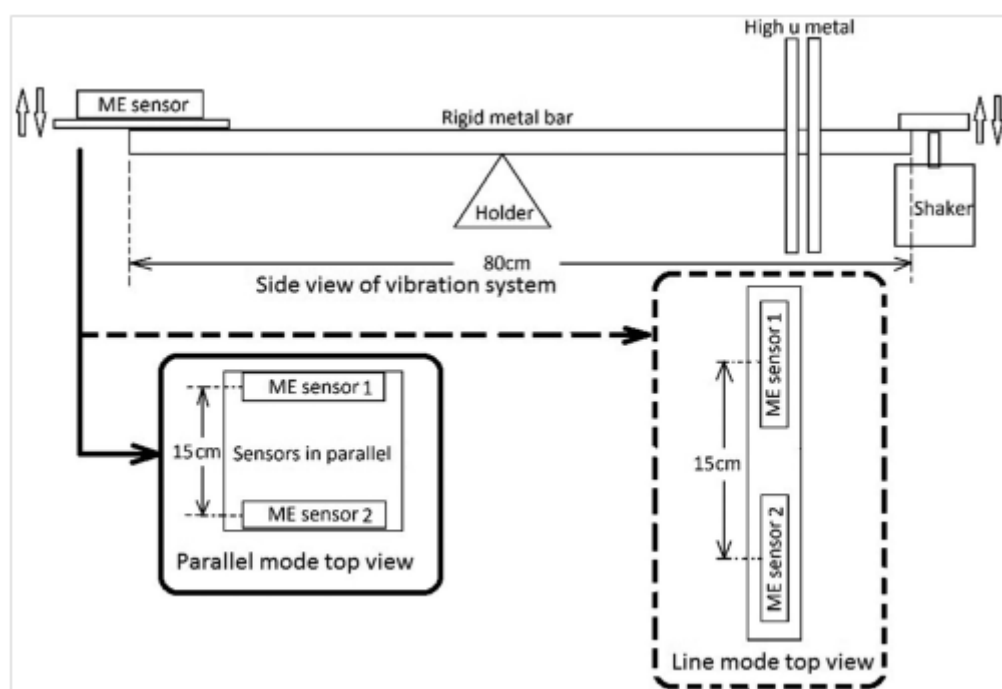


FIG. 13. Vibration rejection measurements of the ME gradiometer based on modulation techniques [70]. Reproduced from *Journal of Applied Physics*, 123, 104501 (2018), with the permission of AIP Publishing.

Recent progress in magnetoelectric energy and power conversion

Energy converters (transducers) are devices which convert one form of energy to another. Energy harvesting is a process that collects/captures the waste energy in an environment (e.g. solar, thermal, mechanical, magnetic and/or electric fields.) and stores it for future usage. A

1
2
3 present interest for collecting/storing energy by harvesting is for powering wireless sensor
4 networks. Typical power consumptions of wireless sensor networks are on the range of micro
5 to milliwatts. Otherwise, wired-powering methods are necessary. ME composites are good
6 energy harvesters in the range of nW to μW range. They can convert energy between magnetic
7 and electrical forms, such as that required to harvest radiated magnetic energy generated by
8 power carrying current cables.
9

10
11
12
13
14 Power conversion can be an electrical, electromechanical, or electromagnetic process for
15 changing the characteristic of electrical energy, such as voltage to current or AC to DC.
16 Conversion can be step-up or step-down. It can be achieved by a rectifier, transformer,
17 voltage/current regulator, and/or gyrator, amongst others possibilities. ME composites
18 combined with copper coils have been demonstrated to be a step-up/down power converter, and
19 more recently as a gyrator that converts current to voltage, or conversely.
20
21
22
23
24

25 In the following paragraphs, ME-based energy harvesting and conversion devices will be
26 discussed. Discussions of ME-based energy harvesters will be divided into two parts: vibration
27 and magnetic. Discussions of power conversion will follow on transformers and gyrators.
28
29
30
31
32
33

34 ME-based Vibration Energy Harvesters

35

36 The first conceptual approach that demonstrated the ME laminates ability to be an energy
37 harvester was reported in 2003 by Huang *et al.* [77]. They proposed that a bipolar magnet
38 changed the direction that flux coupled to the magnetostrictive layers of a ME composite. This
39 was due to vibrations. The relative position between the ME composite and permanent magnet
40 was changed by the external vibration that was incident upon it, resulting in an electrical
41 voltage/power, via the direct ME effect. This energy harvester produced a power of 1 mW under
42 a vibrational acceleration of 2 g at 45 Hz. These results indicated that ME composites could be
43 configured to harvest energy from mechanical vibrations. Numerous investigations of ME-
44 based vibration energy harvesting were then reported. A one-directional bending mode
45 vibration energy harvester was proposed based on tri-layer Terfenol-D/PZT/Terfenol-D ME
46 laminates, which was configured as cantilever beams [78]. The design was based on a
47 piezoelectric cantilever vibration energy harvester driven in a motion by bonded magnets at the
48 end of the cantilever coupling to changes in the magnetic flux. Four NdFeB magnets were
49 alternatively arranged by their poles forming a magnetic yoke. The harvester delivered a
50
51
52
53
54
55
56
57
58
59
60

1
2
3 maximum power output of 1.01 mW at a resonance frequency of 51 Hz under an acceleration
4 of 1 g. Several years later, a similar architecture that employed multiple Terfenol-D/PMN-
5 PT/Terfenol-D tri-layer ME laminates with the same configuration of NdFeB magnets was
6 proposed [79]. The maximum output power before saturation was 1.44 mW at an acceleration
7 of 1 g. However, the harvester produced 7.13 mW at 2.5 g. Both structures were one directional
8 cantilever vibrational energy harvesters.
9
10
11
12

13
14 The cantilever geometry is the most used structure for mechanical energy harvesting of
15 vibrations, basically because of the simple assembly of the structure. However, importantly, a
16 single resonance frequency of the fundamental flexural mode limited the bandwidth for
17 harvesting. Accordingly, a recent trend has been to widen the bandwidth. Therefore,
18 modification using multiple ME transducers to expand the bandwidth have been reported by
19 Yang *et al.* [80] Three cantilever beams, two magnetoelectric laminates, and an alternating
20 NdFeB magnet attached at the free end of the beam were combined to create three natural
21 resonant frequencies, offering an effective bandwidth to the harvester of 7.2 Hz over a
22 resonance range extending from 24 to 20 Hz. It delivered a power of 0.21 mW under an
23 acceleration of 0.2 g. In 2013, Bai *et al.* [81] reported a multi-modal ME vibration energy
24 harvester based on a spiral-shaped cantilever. The spiral cantilever acted as a vibration resonator.
25 Four magnets acted as a proof mass, bonded at the innermost layer of the cantilever. A ME
26 laminate having a (longitudinal-transverse) L - T configuration consisting of two Terfenol-D
27 plates and a single PZT-5H one was fixed at different heights and placed in the middle of the
28 resonator. Under vibration excitation, the spiral cantilever operated in bending and torsional
29 modes, causing the magnets to move relative to the ME laminate. Motion thus occurred in
30 multiple directions producing a complex magnetic field variation. Maximum output powers of
31 118.3, 25.1 80.5, 40.5, and 6.21 μ W were found at different frequencies over the range of 15-
32 70 Hz under an acceleration of 0.2g. In 2016, Lin *et al.* [82] proposed a similar energy harvester,
33 which consisted of a folded cantilever, a ME laminate, and two magnetic circuits. Three ME
34 laminates configured in a L - T mode were arranged and positioned at the tip mass of the
35 cantilever. The harvester was then tested at three different positions, and the results yielded a
36 maximum average power of 31.6 μ W at an acceleration of 0.6 g at a frequency of 13 Hz. Voltage
37 peaks appeared at 13 Hz, 17.4 Hz, and 22.9 Hz, resulting in a working bandwidth of 10.1 Hz.
38
39
40
41
42
43
44
45
46
47
48
49
50
51
52
53
54
55

56 Most energy harvesting devices collect power in a unidirectional mode. They lack the
57 ability to harvest vibrations from other directions. To overcome this limitation, bi-axial ME
58 vibration energy harvesters have been developed that utilize multiple cantilevers to extract
59
60

1
2
3 vibration energy from multiple directions. In 2012, Yang *et al.* [83] proposed a harvester that
4 consisted of two cantilevers and two ME laminates. The ME laminates were attached at the end
5 of the two cantilevers as tip masses and consisted of a *L-T* structure of Terfenol-D bonded to
6 PMN-PT. These two cantilevers were then mounted along vertical directions and placed inside
7 a four-alternatively poled permeant magnet configuration. The energy harvester had
8 bandwidths of 2.8 Hz and 2.5 Hz along vertical and horizontal directions under a vibration
9 acceleration of 0.6 g, and the maximum output voltage was 130 V. In the same year, Moss *et*
10 *al.* [84] proposed a bi-axial ME energy harvester using a permanent-magnet/ball bearing
11 arrangement, together with a ME laminate composite. The ME laminate was formed by bonding
12 two Terfenol-D plates and a PZT layer into a *L-T* mode structure. The magnetic flux distribution
13 in the ME composite was changed when the ball bearing oscillated with a restoring force on the
14 ball, and when it was free to move on the surface of the upper magnetostrictive layer. Under an
15 external acceleration vibration of 61 mg at 9.8 Hz, a maximum power output of 121 μW was
16 achieved. Although the harvested power was relatively small, the vibration region of the ball
17 bearing was relatively free to move, enabling the harvester to collect vibration energy in
18 multiple directions.
19
20
21
22
23
24
25
26
27
28
29

30
31 Bandwidth and multi-directionality are two of the most important issues in the
32 development of vibration energy harvesting. All previous designs could not overcome both
33 these limitations at the same time. In 2016, Lin *et al.* [85] reported a 3-directional ME harvester
34 consisting of a cylindrical magnet mounted by three springs, three ME laminates, and a
35 mounting frame. The three springs and ME laminates were mounted symmetrically on the frame
36 at an angle of 120° , and the angle between the springs and laminates was 60° . Under external
37 vibrations, the relative motions of the center cylindrical magnet produced various magnetic
38 field variations in arbitrary directions, enabling the direct ME effect of the ME laminate to
39 harvest an electrical power. Different out-of-plane and in-plane vibration experiments were
40 tested at different angles to confirm the harvesting ability in multi-directions. Experiments
41 showed that a maximum load power of 12.9 μW could be achieved over a wide bandwidth of
42 3.2 Hz at a natural resonance frequency of 10 Hz and under an acceleration of 1g. The schematic
43 diagram of discussed multi-directional vibration-typed ME energy harvester is shown in Fig. 14.
44
45
46
47
48
49
50
51
52
53
54
55
56
57
58
59
60

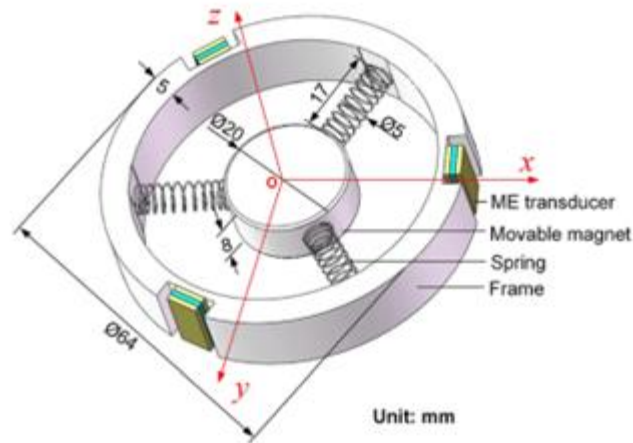


Fig.14. A central cylindrical magnet mounted by three identical springs inside a ring frame which attached with three ME transducers located in a 120° arrangement [85]. Reproduced from *Applied Physics Letters*, 109, 253903 (2016), with the permission of AIP Publishing.

In recent years, researchers have put much effort into different designs to enhance the energy harvesting performance of ME composites. In 2012, Zhu *et al.* [86] proposed an energy harvester based on L - T laminates, which was fixed to the surface of a center pole. Two magnets were fixed at the top and bottom of the pipe's outer surface, allowing the middle magnet to be free to move and levitate. Experiments showed a maximum power output of 1.1 mW under a vibration acceleration of 1 g at 10 Hz. In 2013, Li *et al.* [87] reported a passive self-tuning energy harvester for collecting energy in rotating applications. The mechanical energy harvester had two hollow magnets with ME laminates placed inside the holes, and two cylindrical magnets mounted on the free end of a cantilever beam that was placed between the two free moving hollow magnets. The core ME laminate was formed by two Terfenol-D and one PMN-PT plates with a L - T configuration. By changing the distance between the magnets on the cantilever beam and the ME laminate, the power, voltage, vibration displacement, and frequency could all be tuned. The harvester was then mounted on a wheel driven by an ac servo-actuator. Experiments found that a maximum power of 517 μ W could be harvested at a rotation frequency of 9.8 Hz. Recently, in 2016, Dai *et al.* [88] proposed an energy harvester composed of a L - T ME laminate and a rotary pendulum embedded with six magnets. The rotary pendulum was mounted on a supporting fixture using a bearing, and the ME laminate was placed between the magnets. This prototype produced a 3dB bandwidth of 3.2 Hz and an output power of 970.2 μ W under an acceleration of 0.5 g at 14.8 Hz.

ME-based magnetic harvesters

Magnetic field or electric power line energy harvesting is an alternative use for the ME effect, such as the radiated magnetic energy generated from a power/current cord or line. To harvest this magnetic energy, in 2004, Bayrashev *et al.* [89] developed a disk-shaped sandwich ME laminate constructed by a PZT layer sandwiched between two Terfenol-D ones. This laminate was then placed near a permanent magnet that was attached to the shaft of a linear variable frequency (1-30 Hz) motor. The resulting output power was found to be 10-80 μW , depending on the distance between the ME laminate and permanent magnet.

In 2010, Wang *et al.* [90] characterized the effect of an electrical resistance load on the ME coupling using a *L-T* mode Terfenol-D/PMN-PT/Terfenol-D ME laminate. The output power initially increased with increasing resistance load at resonance, reached a maximum value, and then decreased with further increase of resistance load. This observation was similar to that for systems using PZT type ME laminates connected with various load resistances. The results demonstrated that the proposed laminate was capable of producing 1.9 mW at a resonance frequency of 83.6 kHz.

One of the biggest challenges for practical application of ME laminates has been their relatively high resonance frequency which limits their application in energy harvesting from industrial/household electrical devices. In the real world, the frequencies of the electric power delivered are in the range of 50/60 Hz. Thus, it is highly desirable to tune the resonance frequency to considerably lower frequency ranges, in order to optimize the output power from ME harvesters. In 2012, Gao *et al.* [91] demonstrated a tunable unsymmetrical bi-layer Metglas/PZT ME composite that harvested 60 Hz electromagnetic energy. By attaching different numbers of permanent magnets as tip masses, the resonance frequency could be adjusted from 60 to 220 Hz. The optimized output power of this harvester reached 16 $\mu\text{W}/\text{Oe}$ at a resonance frequency of 60 Hz after tuning the tip mass. This demonstrates a simple and direct way to use ME laminates to harvest the magnetic energy generated by current carry cables. In the same year, Qiu *et al.* [92] reported a design for energy harvesters based on a ME bending configuration, allowing for significant reduction in device size. It consisted of cantilever beams, ME transducer, and a magnetic yoke configured by permeant magnets. A PZT -plate was bonded to the cantilever beam and fixed on a holder. An electric cable was placed in the center of the magnetic yoke and fixed to a support. When a current passed through the electric cable, an alternating force was generated via Ampere's law between current and magnetic field. Since

the cable line was fixed to the holder, this force acted on the cantilever, causing it to vibrate and deform. An output power of $240 \mu\text{W}$ was generated in response to an input current of 3A at 50 Hz.

A Halbach magnet array is a special arrangement of permanent magnets that enhances the magnetic field on one side of an array. A Halbach magnet mounted on the end of a cantilever has been employed with an L - T mode Terfenol-D/PZT/Terfenol-D ME laminate to enhance the harvested power [93]. The results showed an output power of $523\mu\text{W}$ under an electric current of 5A at 50 Hz. Commonly two wires (live and neutral) are combined in a cord that is required to carry power to an appliance. The two wires are bundled parallel and placed close together, then a magnetic field from one will near-exactly cancel that from the other. Accordingly, a special design is required to overcome this limitation and to enhance the performance. In 2006, Leland *et al.* [94] proposed an energy harvesting device constructed from cantilever-mounted piezoelectric bimorphs and permanent magnets. It was able to harvest the radiated magnetic power from two such conductor power cables. A maximum power output of $208 \mu\text{W}$ under 9.4A and $345 \mu\text{W}$ under 13 A (60 Hz) was found. In 2014, He *et al* [95] fabricated a similar bending mode ME harvester, designed for two-wire power cords. This energy harvester had a magnetic circuit consisting of six alternately poled NdFeB magnets mounted on the free end of a cantilever beam and a L - T trilayer structure of Terfenol-D/PMN-PT/Terfenol-D. Because of the opposite arrangement of magnets, the Ampere forces acting on the two conductors were superimposed. This resulted in an enhanced maximum power of $671.2 \mu\text{W}$ under a current of 6A at 50 Hz. All schematic diagrams, photos, and resulted output power of previous ME-based magnetic harvesters are shown in Fig. 15.

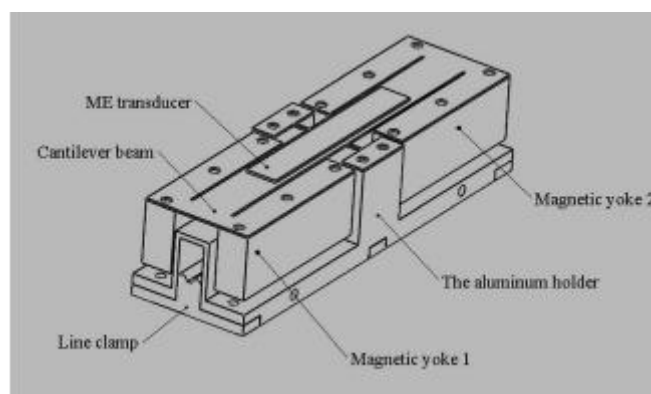


Fig. 15. Schematic diagram of the piezoelectric cantilever beam and ME transducer based magnetic field-current energy harvester for single core power cable [92]. Reproduced from *Journal of Applied Physics*, 111, 07E510 (2012), with the permission of AIP Publishing.

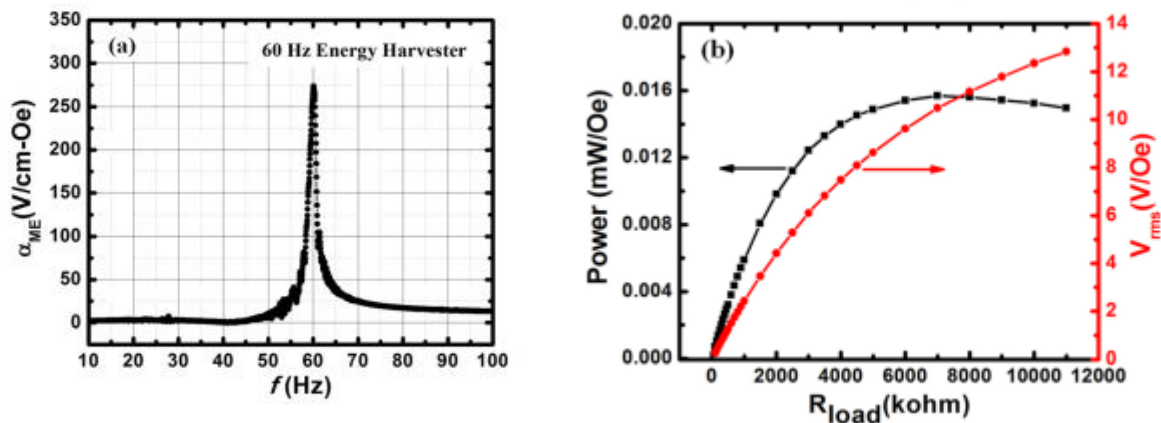


Fig. 16. (a) ME voltage coefficient of 60 Hz magnetic energy harvester as a function of AC magnetic drive frequency and (b) output voltage and power as a function of resistance load at the bending mode resonance frequency [91]. Reproduced from *Journal of Applied Physics*, 112, 104101 (2012), with the permission of AIP Publishing.

Unused power, which can be harvested from industrial machine/transportation vehicles is usually available as either vibration or magnetic fields. To enhance the power harvesting density, multimodal ME energy harvesters with various configurations that combined both vibration and magnetic harvesting mechanism were proposed by Dong *et al.* [96] in 2008. A ME laminate can be configured to harvest vibration and magnetic energies at the same time using the direct ME and direct piezoelectric effects. This was achieved by configuring the ME laminate from two push-pull symmetrically poled PZT fibers laminated together with four FeBSiC ribbons as shown in Fig. 17. The first longitudinal resonance frequency of the ME laminate was 21 kHz without any mechanical vibration input, and the output power was 520 μW under 1 Oe. However, in an open ambient environment, there are limited sources of emitted magnetic flux in this 20 kHz frequency range. A cantilever beam structure with a tip mass was thus used to lower the frequency range to between 20 and 40 Hz. A peak-to-peak output voltage of 8 V was obtained from both piezoelectric layers under a magnetic field of 2 Oe together with a vibration of 0.05 g. This output voltage was doubled relative to a single power source, proving the possibility to harvest both vibration and magnetic field energies simultaneously. A flexible, low-cost energy-harvesting device based on the magnetoelectric (ME) effect was designed using $\text{Fe}_{64}\text{Co}_{17}\text{Si}_7\text{B}_{12}$ as amorphous magnetostrictive ribbons and polyvinylidene fluoride (PVDF) as the piezoelectric element by Lasheras *et al.* [97] in 2015. A 3 cm-long sandwich-type laminated composite was fabricated by gluing the ribbons to the PVDF with an epoxy resin. A voltage multiplier circuit was designed to produce enough voltage to charge a battery. The power output and power density obtained were 6.4 μW and 1.5 mWcm^{-3} , respectively, at optimum load resistance and measured at the magnetomechanical resonance of the laminate.

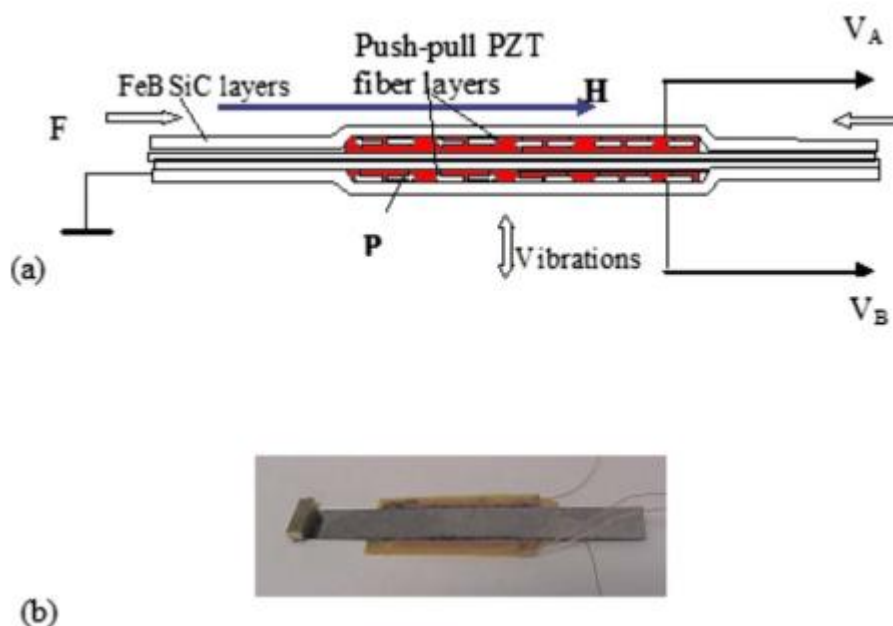


Fig. 17. Conceptual illustration of the ME energy harvester: (a) schematic of the ME laminate configuration with p polarization units and (b) photo of the ME laminate prototype, [96]. Reproduced from *Applied Physics Letters*, 93, 103511 (2008), with the permission of AIP Publishing.

Previous investigations have shown that the resonance frequency of ME beam harvesters can be reduced by changing the operational modes of the harvesting system. However, this additional mechanical load is also a damping term that reduces the efficiency of the harvester. To avoid this problem, in 2013, Zhou *et al.* [98] reported a dual-phase energy harvester. It was configured by combining a ME laminate and a piezoelectric unimorph bonded in a cantilever structure. The piezoelectric layer was a micro-fiber composite (MFC) bonded to a nickel cantilever beam. The schematic diagram self-bias dual-phase energy harvester is shown in Fig. 18. This cantilever not only served as a magnetostrictive phase to transfer the stress and strain to the piezoelectric layer, but also as a bender for vibrations to directly create strain in the piezoelectric layer. Under a vibration acceleration of 0.17 g at 22.5 Hz, the harvester induced a maximum electrical power output of 168 μ W. Under this hybrid approach (magnetic and vibration), they found that the vibration energy was the main contributing at a frequency of 22.5 Hz.

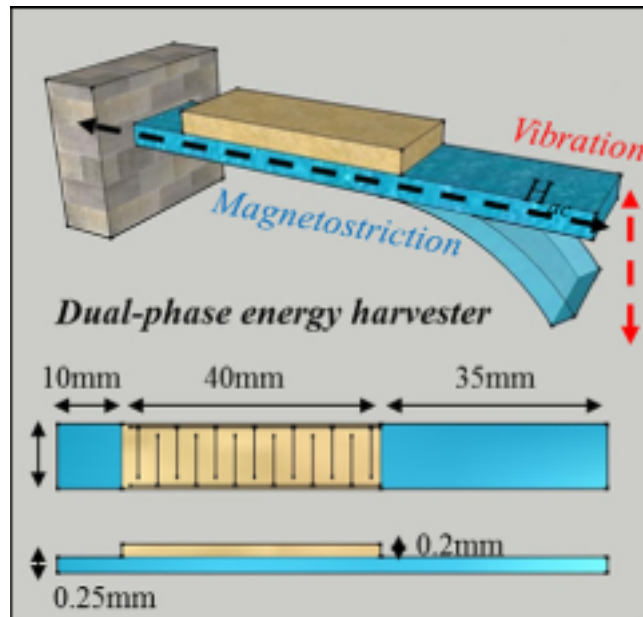


Fig.18. Schematic diagram of self-bias dual-phase energy harvester consisting of magnetostrictive bender and ME composite [98]. Reproduced from *Applied Physics Letters*, 103, 192909 (2013), with the permission of AIP Publishing.

In 2015, Qiu *et al.* [99] proposed a vibration-based energy harvester that hybrid ME and electromagnetic sources. It consisted of a magnetic circuit combined with four permanent magnets, a hybrid transducer combined with a coil-wrapped five-phase ME laminate and a cantilever. All components were fixed on an aluminum holder and mounted on a shaker for testing. The five-phase ME laminate was composed of *L-T* FeCuNdSiB/Terfenol-D/PZT/Terfenol-D/FeCuNdSiB configuration. A maximum output power of 40.84 mW was found at a resonance frequency of 25.7 Hz under an acceleration of 0.75g.

ME-based transformers/gyrators

Similar to a conventional magnetic transformer, ME laminates can be used as a step-up/down transformer, which transforms an ac voltage/current at the primary/input side to a proportional voltage/current at the secondary/output side. Such ME step-up or down converters have the potential to replace conventional transformers at their lower power levels, as they have smaller sizes and weight. In 2004, our team [100] observed a large gain effect in a ring-type ME laminate. It consisted of two circumferentially magnetized Terfenol-D rings and a circumferentially poled PZT one (consisting of 4 segments) wrapped with a toroidal coil. When an ac voltage was applied to the coil, an ac current flowed into the coil, subsequently creating a vortex magnetic field of the same frequency along the circumference direction of the laminate. Based on a direct ME effect under resonance drive, a higher voltage output was obtained in the

1
2
3 piezoelectric layers. A maximum voltage gain of $25\times$ was found under a magnetic bias of 500
4 Oe at 53.3 kHz. These findings demonstrated the feasibility that ME laminates could be used
5 as a solid-state step-up power converter. In 2004, our team [101] found an extremely high
6 voltage gain effect of ≈ 300 in a rectangular-shaped ME laminate. The geometry was a long
7 longitudinally poled push-pull piezoelectric layer sandwiched between two longitudinally
8 magnetized Terfenol-D plates. By taking advantages of a high mechanical quality factor and
9 the longitudinally poling of PZT, a maximum voltage gain of $260\times$ was achieved at a resonance
10 frequency of 21.3 kHz. A few years later, in 2009, Wang *et al.* [102] reported a large voltage
11 gain of 130 at resonance using a long-type ME heterostructure consisted a length magnetized
12 Terfenol-D layer and a length-polarized PMN-PT one. A detailed study of the voltage gain and
13 output power from the converter as a function of resistive load confirmed that a similar load
14 effect was observed as for piezoelectric transformers. The detailed structure of ME transformer
15 configured in ring and sandwich were shown in Fig. 19.
16
17
18
19
20
21
22
23
24
25
26
27
28
29
30
31
32
33
34
35
36
37
38
39
40
41
42
43
44
45
46
47
48
49
50
51
52
53
54
55
56
57
58
59
60

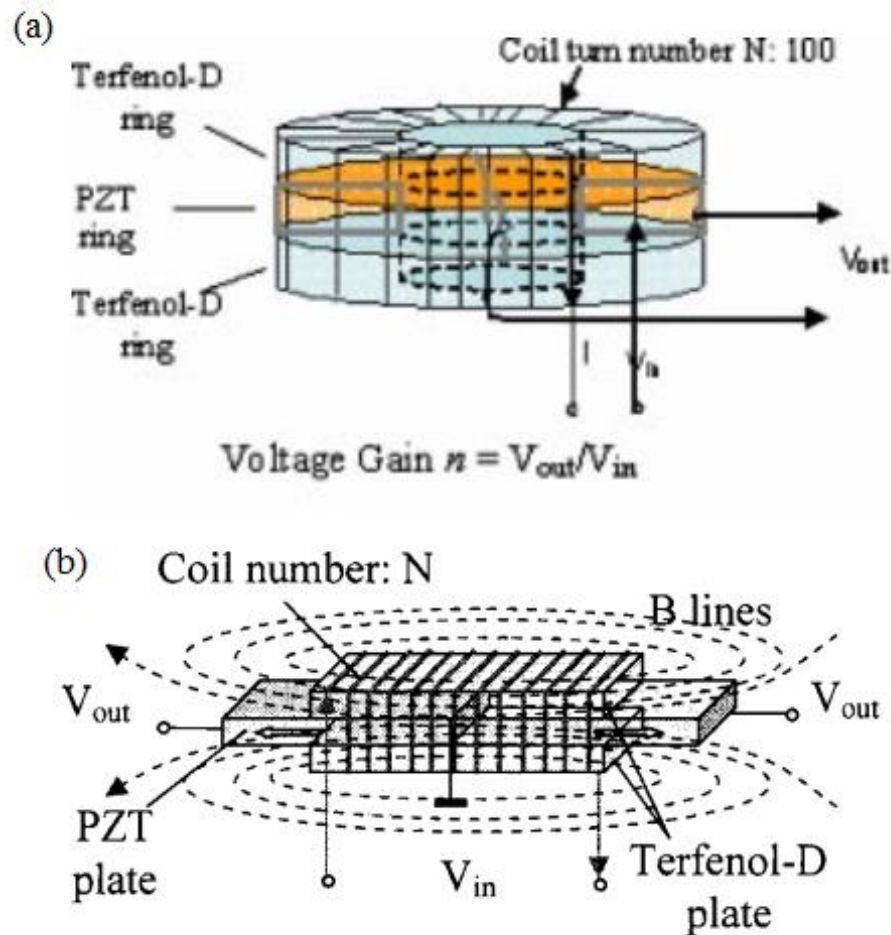
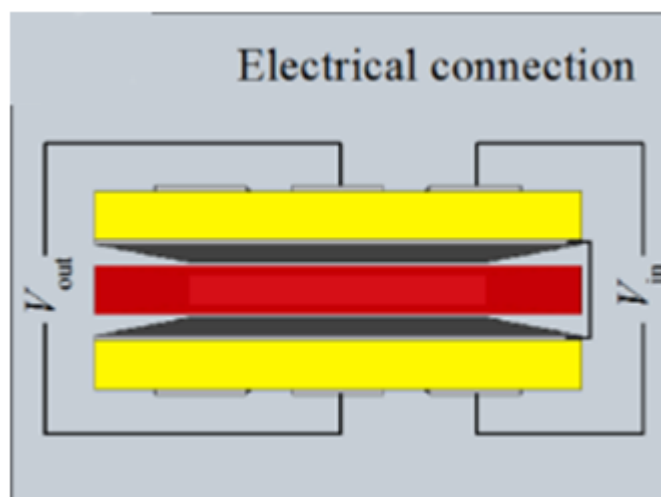


Fig.19. Different structures of ME transformer in (a) ring-type and (b) sandwich-type [100,101]. Reproduced from *Applied Physics Letters*, 84, 4188–90 (2004) and *Applied Physics Letters*, 85, 3534–6 (2004), with the permission of AIP Publishing.

Due to the resonance feature of ME-based laminates with a high-quality factor, they have potential applications as step-up/down converters in power electronics. The gain characteristics of ME converters are highly dependent on load and are useful only over a narrow frequency range near resonance. This has led to some challenges in design that require evaluation for a range of applications. Tunable ME gain effects and external magnetic fields have potential usefulness. In 2009, our team [18] made a tunable ME transformer that combined FeBSiC alloy ribbons and a piezoelectric PZT fiber operated in a push-pull mode. This laminate composite was wrapped by a copper coil that served as an input port. Because of the low magnetic bias field required for FeBSiC foils, a linear tunable voltage gain occurs under small magnetic bias changes between -5 and 5 Oe, where the maximum voltage gain of 55 was found under 5 Oe at resonance. In 2011, using the same DC magnetic field tunable properties in the magnetostrictive layer, Lv *et al.* [103] made a new type of ME transformer that combined a

1
2
3 traditional Rosen-type piezoelectric transformer and a Terfenol-D plate. This allowed the
4 voltage gain of the piezoelectric transformer to be controlled by dc magnetic bias fields. Two
5 sharp peaks in the voltage gain were found. A maximum gain of 7.7 was found under zero
6 magnetic bias that was enhanced to 9.2 V under 2500 Oe. Later, Zhou *et al.* [104] proposed a
7 co-fired type ME transformer that consisted of two unipoled PZN-PT transformers and a nickel-
8 zinc copper (NZCF) ferrite layer (Fig. 20). This co-fired ME transformer exhibited a large
9 frequency tunability effect. Although a voltage gain of only 1.52 was found at resonance
10 without magnetic bias, a large frequency tunability of 1.4 Hz/Oe was achieved under bias,
11 opening up the possibility of developing on-chip converters for electronics.
12
13
14
15
16
17
18
19
20
21



22
23
24
25
26
27
28
29
30
31
32
33
34
35
36
37
38 **Fig. 20. Schematic diagrams of (a) co-fired PZNT/Ag/NZCF/Ag/PZNT laminate structure [104].** Reproduced
39 from *Applied Physics Letters*, 104, 232906 (2013), with the permission of AIP Publishing.
40

41
42 Two-port four-wire ME laminates with lumped or distributed components may have
43 applications such as transformers, waveguides, and antennas. The voltage to current
44 relationship between inputs and outputs offer, for example, voltage-to-current conversions and
45 maximum power transfer efficiency. Such network elements have characteristic expected of a
46 gyrator. The gyrator was first conjectured by Tellegen [40] in 1948 to be a missing fifth network
47 circuit element. It may be considered to be a two-port four-wire circuit which has the property
48 that the phase shift for transmission in one direction differs by 180 degrees from that for
49 transmission in the other direction. Another property is impedance inversion between the input
50 and output ports, which provide unique current-to-voltage/voltage-to-current features. A
51 conceptual diagram of ME gyrators was given in Fig.7. In 2006, our team [41] demonstrated
52 that a L - T Terfenol-D/PZT/Terfenol-D tri-layer laminates wrapped with a 50-turn copper wire
53
54
55
56
57
58
59
60

had characteristics similar to gyrator properties. The investigation revealed a 180-degree phase shift at low frequencies, whose phase changed rapidly near resonance, and a large non-dissipative I - V conversation feature at resonance. In 2009, we reported a more detailed study of ME gyrators based on Terfenol-D/PZT/Terfenol-D, Metglas/PZT/Metglas, and Ni/PZT/Ni [105]. Experimental results showed that the Metglas based gyrators had superior power conversion ability, relative to Terfenol-D and Ni of similar dimensions [106]. These gyrators were configured with L - T tri-layer structures. This study also reported conversion characteristics of capacitance to inductance, and impedance inversion. The voltage and current transfer relationships were discussed using the following impedance matrix given as [41]

$$Z = \begin{bmatrix} Z_{11} & Z_{12} \\ Z_{21} & Z_{22} \end{bmatrix} = \begin{bmatrix} R_{11} & R_{12} \\ R_{21} & R_{22} \end{bmatrix} + j \begin{bmatrix} X_{11} & X_{12} \\ X_{21} & X_{22} \end{bmatrix};$$

where R and X are the real and imaginary parts of the impedance. The ratio between the impedances Z_{21} and Z_{12} should be 1, in order to guarantee an ideal gyrator. This leads to an equality of $\frac{\alpha_{ME}}{\sqrt{\epsilon_r \mu_r}} = 1$, where α_{ME} is the magnetoelectric susceptibility and ϵ_r and μ_r are the effective permittivity and permeability in ME composite.

In particular, the step-up/down I - V / V - I conversion features of ME laminates wrapped with a coil offers much potential as a ME gyrator. In 2009, our team [18] reported a ME transformer with tunable features using FeBSiC Metglas and hard PZT layers, which had an efficiency less than 50%. The low efficiency was conjectured to be caused by various loss factors such as copper coil loss, Eddy current loss, dielectric loss and frictional loss imposed by the bonding layer (epoxy). A piezoelectric material with a high mechanical quality factor, Metglas foils with a higher resistivity, and an elastically matching bonding layer (different thickness ratios) have been suggested as approaches to improve the efficiency [18]. However, the power conversion characteristics of ME gyrators were not studied in detail, until 2016, when Leung *et al.* [107] reported the power conversion efficiency of a coil-ME gyrator based on Terfenol-D/PZT L - T laminates. A detailed experimental setup is outlined in Fig. 21. The maximum values of the current-to-voltage coefficient was 1454 V/A and the correspond voltage-to-current one was 0.468 mA/V, when operated at resonance. In this study, a power efficiency of 35% was found in both direct and converse modes. These findings showed that ME gyrators have power conversion characteristics that offer an approach to replace conventional electromagnetic and piezoelectric transformers. Such a low power efficiency of

35% would limit the application of ME gyrators as power converters. However, theoretical predictions indicated that ME composites should be capable of having power conversion efficiencies of greater than 90% [108].

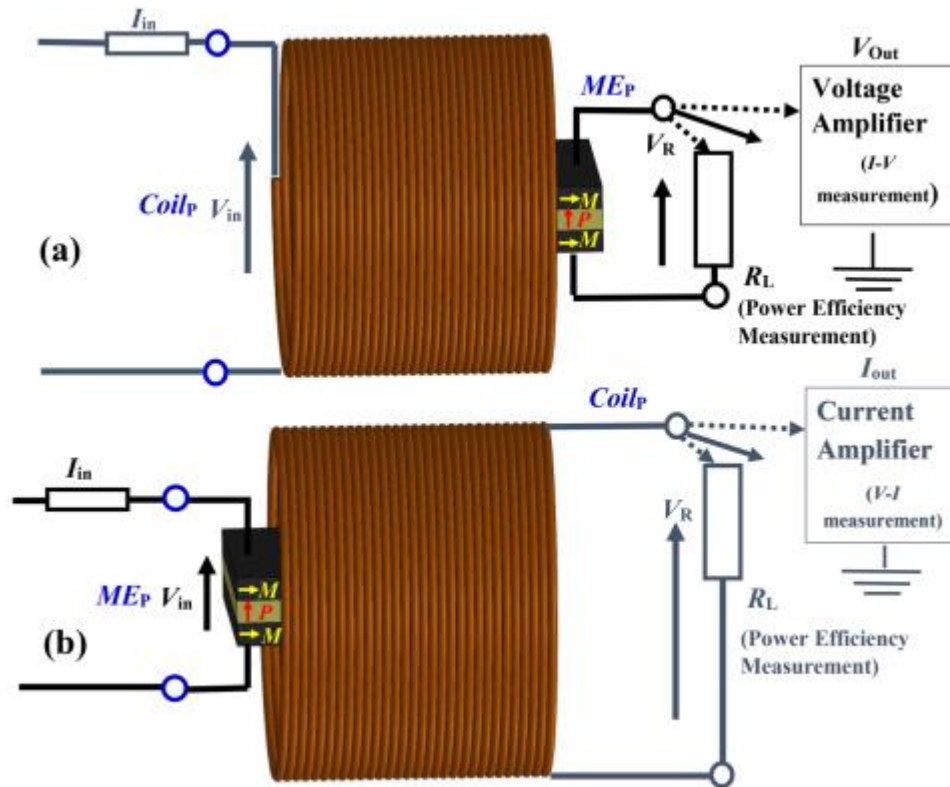


Fig.21. (a)I-V, (b)V-I, and (direct and converse) power efficiency measurement setup for ME gyrators [107]. Reproduced from *Applied Physics Letters*, 109, 202907 (2016), with the permission of AIP Publishing.

The path to improving the power efficiency (η) of ME gyrators was to increase the product of the square of the effective coupling factor in the magnetostrictive phase ($k_{eff,m}^2$) and the mechanical quality factor of the ME laminate (Q_{mech}). Improvements in the power conversion efficiency of ME gyrators then focused on this important $k_{eff,m}^2 Q_{mech}$ product [109]. Experimental investigations have confirmed that both high $k_{eff,m}$ and Q_{mech} are important factors for increasing η . In 2017, Leung *et al.* [110] reported another important parameter that affected the power efficiencies of ME gyrators. For Terfenol-D/PZT/Terfenol-D tri-layers, the efficiency was found to be increased by decreasing the thickness/volume ratio between Terfenol-D and PZT phases. This is because the average mechanical quality factor was increased by decreasing the ratio of Terfenol-D in the ME laminate: Q_{mech} of PZT was ~ 500 , whereas that of Terfenol-D was ~ 7 . Investigations showed that the volume fraction of the Terfenol-D magnetostrictive layer was the main limitation of η for ME gyrators. NZFO was then proposed to replace the Terfenol-D layer in ME gyrators, in order to reduce the magnetic

1
2
3 core loss due to Eddy currents. NZFO has a much small Eddy current loss, and also has a high
4 magnetostriction [28].
5
6

7
8 Our research team then experimentally identified the loss mechanism of ME gyrators by
9 using a transformer-gyrator structure [111]. At low power conditions, an optimal (but not
10 matched) load resistor reflected a portion of the power. This was revealed as a decrease in the
11 magnetomechanical conversion efficiency in the magnetostrictive phase. Under high power
12 conditions, a portion of the power was transformed back to its pure magnetic form and captured
13 as a leakage power by the secondary coil.
14
15
16
17

18
19 A high power density of 60 Watt/in³ has recently been achieved for a Metglas/PZT
20 gyrotor [111]. This makes ME gyrators promising devices for high power applications. η was
21 also increased to 85% for nickel-zinc ferrite/PZT ME gyrators at low power conditions
22 (~20 mW/in³), and $\geq 80\%$ at higher power conditions (~5 W/in³). This increase was due to the
23 high mechanical quality factor of the ferrite [28]. Next, piezoelectric-magnetostrictive-
24 piezoelectric (P-M-P) trilayer structures were designed. The P-M-P structure resulted in
25 enhanced power efficiency stability for the ferrite-based gyrators with increasing power density,
26 reaching an efficiency of 79% under 47Watt/in³ [112]. The magnetomechanical conversion
27 efficiency was directly measured as a function of power density [113], revealing that both
28 Metglas and ferrites have extremely high magnetomechanical conversion efficiencies under
29 low power conditions. However, it was found that Metglas can retain its superior efficiency at
30 higher power drive conditions than ferrite. By using a piezoelectric material with a high
31 mechanical quality factor, an optimal thickness ratio and a matching length of the coil to ME
32 composite, a high power efficiency of greater than 90% was first achieved by
33 Zhuang *et al.* [113].
34
35
36
37
38
39
40
41
42
43
44
45
46
47
48
49
50
51
52
53
54
55
56
57
58
59
60

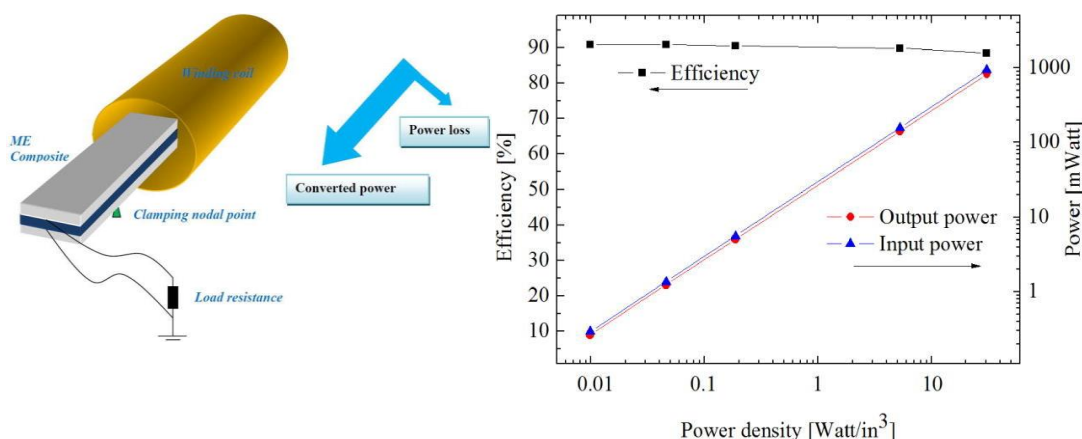


Fig. 22. Structure and power performance of Metglas/PZT gyrators [113]. Reproduced from *Applied Physics Letters*, 111, 163902 (2017), with the permission of AIP Publishing.

Under high drive conditions, the efficiency of Metglas/PZT gyrators have been found to retain their superiority ($\eta=89\%$) up to power densities of 30Watt/in^3 , as shown in FIG. 23, offering the potential to realize ME gyrators in applications as power electronic devices. The Metglas used in this ME configuration was annealed resulting in a minor volume fraction of Fe nano-crystallites, and it also contained manganese and carbon dopants (FeCoSiBMnC). Both the Metglas and PZT phases were hardened to achieve extraordinarily high mechanical quality factors of ~ 1000 . Figure 28 summarizes a list of the significant investigations of power density and power efficiency for ME gyrators with different material combinations in Refs [18,107,110,111,28,113,112], respectively.

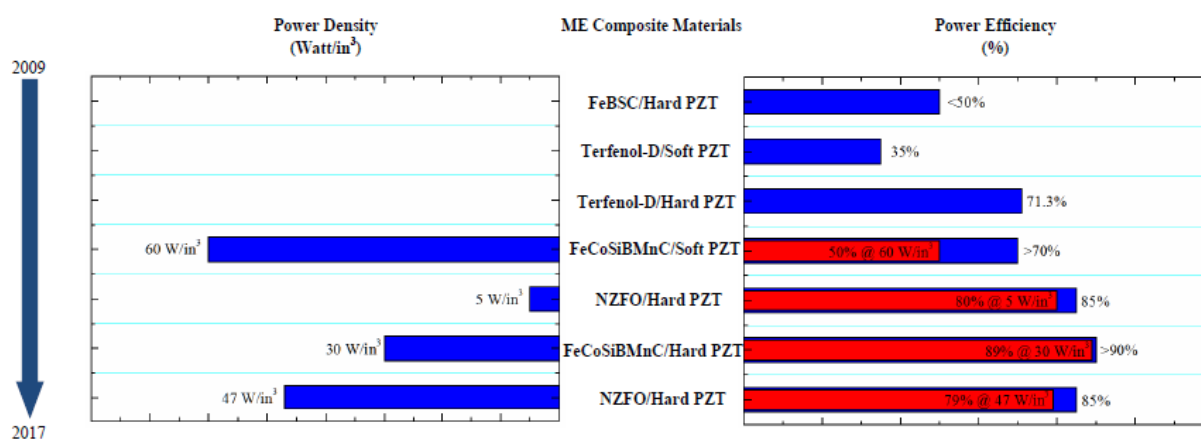


Fig. 23. Reported maximum values of power density and power efficiency for various type materials in Refs [18,107,110,111,28,113,112], respectively.

Conclusion

The focus of this review was on recent progress in ME composites and their applications from low to high power conditions. It is difficult to cover all ME materials that have recently been developed. Recent research activities on macro ME composites was discussed. Many investigations have advanced these materials towards real-world applications. These applications include magnetic sensors, energy harvesters, and power converters. Starting with a brief summary of the history of the ME effect, the paper then focused on the recent development of macro ME composites and their applications, as well their figures of merit. Non-resonant and resonant enhancements of the ME coefficients were discussed for various magnetostrictive (e.g. ferrites, transition metals, and alloys) and piezoelectric phases. The development of the ME sensors based on the selection of material properties and fabrication methods have been discussed, which resulted in a new type of magnetic sensors with minute power consumption and extremely high detection performance, which are competitive to existing magnetic sensor. Different ME-based energy harvesters have been compared according to their directionality, bandwidth, and sources of energy. Finally, a summary of recent advances in gyrators based on ME composites has been included in this review. The voltage/current step-up/down ratios and the power performances, involving power efficiency and power density, have been presented and discussed, which offer the ME gyrator as a potential electronic device for power conversion applications. We believe that ME composites offer the potential to unleash applications of non-destructive detections [114], power controlling systems in smart grids [115], wireless power transmission [116], and communications [117]. This promising potential is enabled by the high ME coupling that is unique to ME laminates and their devices.

Acknowledgements

This work was supported by the Defense Advanced Research Projects Agency through the MATRIX Program, grant number W911NF-15-1-0616.

Reference

- [1] Röntgen W C 1888 Ueber die durch Bewegung eines im homogenen electrischen Felde befindlichen Dielectricums hervorgerufene electrodynamische Kraft *Ann. Phys.* **271** 264–70
- [2] Curie P 1894 Sur la symétrie dans les phénomènes physiques, symétrie d'un champ électrique et d'un champ magnétique *J. Phys. Théorique Appliquée* **3** 393–415
- [3] Debye P 1926 Bemerkung zu einigen neuen Versuchen über einen magneto-elektrischen Richteffekt *Z. Für Phys.* **36** 300–1
- [4] Astrov D N 1960 The magnetoelectric effect in antiferromagnetics *Sov Phys JETP* **11** 708–9
- [5] Astrov D N 1961 Magnetoelectric effect in chromium oxide *Sov Phys JETP* **13** 729–33
- [6] Fiebig M 2005 Revival of the magnetoelectric effect *J. Phys. Appl. Phys.* **38** R123
- [7] Ma J, Hu J, Li Z and Nan C-W 2011 Recent Progress in Multiferroic Magnetoelectric Composites: from Bulk to Thin Films *Adv. Mater.* **23** 1062–87
- [8] Eerenstein W, Mathur N D and Scott J F 2006 Multiferroic and magnetoelectric materials *Nature* **442** 759
- [9] Nan C-W, Bichurin M I, Dong S, Viehland D and Srinivasan G 2008 Multiferroic magnetoelectric composites: Historical perspective, status, and future directions *J. Appl. Phys.* **103** 031101
- [10] Velev J P, Jaswal S S and Tsymbal E Y 2011 Multi-ferroic and magnetoelectric materials and interfaces *Philos. Trans. R. Soc. Lond. Math. Phys. Eng. Sci.* **369** 3069–97
- [11] Van Suchtelen J 1972 Product properties: a new application of composite materials *Philips Res Rep* **27** 28–37
- [12] Boomgaard J V D, Terrell D R, Born R a. J and Giller H F J I 1974 An in situ grown eutectic magnetoelectric composite material *J. Mater. Sci.* **9** 1705–9
- [13] Ryu J, Carazo A V, Uchino K and Kim H-E 2001 Magnetoelectric Properties in Piezoelectric and Magnetostrictive Laminate Composites *Jpn. J. Appl. Phys.* **40** 4948
- [14] Dong S, Li J-F and Viehland D 2003 Longitudinal and transverse magnetoelectric voltage coefficients of magnetostrictive/piezoelectric laminate composite: theory *IEEE Trans. Ultrason. Ferroelectr. Freq. Control* **50** 1253–61
- [15] Dong S, Li J-F and Viehland D 2004 Longitudinal and transverse magnetoelectric voltage coefficients of magnetostrictive/ piezoelectric laminate composite: experiments *IEEE Trans. Ultrason. Ferroelectr. Freq. Control* **51** 794–9
- [16] Zhai J, Dong S, Xing Z, Li J and Viehland D 2006 Giant magnetoelectric effect in Metglas/polyvinylidene-fluoride laminates *Appl. Phys. Lett.* **89** 083507

- 1
2
3 [17] Dong S, Zhai J, Li J and Viehland D 2006 Near-ideal magnetoelectricity in high-
4 permeability magnetostrictive/piezofiber laminates with a (2-1) connectivity *Appl.*
5 *Phys. Lett.* **89** 252904
6
7 [18] Dong S, Zhai J, Priya S, Li J F and Viehland D 2009 Tunable features of
8 magnetoelectric transformers *IEEE Trans. Ultrason. Ferroelectr. Freq. Control* **56**
9 1124–7
10
11 [19] Wang Y, Gray D, Berry D, Gao J, Li M, Li J and Viehland D 2011 An Extremely Low
12 Equivalent Magnetic Noise Magnetoelectric Sensor *Adv. Mater.* **23** 4111–4
13
14 [20] Gao J, Shen L, Wang Y, Gray D, Li J and Viehland D 2011 Enhanced sensitivity to
15 direct current magnetic field changes in Metglas/Pb(Mg_{1/3}Nb_{2/3})O₃–PbTiO₃
16 laminates *J. Appl. Phys.* **109** 074507
17
18 [21] Lasheras A, Gutiérrez J and Barandiarán J M 2017 Size effects in the equivalent
19 magnetic noise of layered Fe₆₄Co₁₇Si₇B₁₂/PVDF/Fe₆₄Co₁₇Si₇B₁₂ magnetoelectric
20 sensors *Sens. Actuators Phys.* **263** 488–92
21
22 [22] Wang Y, Gray D, Gao J, Berry D, Li M, Li J, Viehland D and Luo H 2012
23 Improvement of magnetoelectric properties in Metglas/Pb(Mg_{1/3}Nb_{2/3})O₃–PbTiO₃
24 laminates by poling optimization *J. Alloys Compd.* **519** 1–3
25
26 [23] Kirchoff C, Krantz M, Teliban I, Jahns R, Marauska S, Wagner B, Knöchel R, Gerken
27 M, Meyners D and Quandt E 2013 Giant magnetoelectric effect in vacuum *Appl. Phys.*
28 *Lett.* **102** 232905
29
30 [24] Chu Z, Shi H, Shi W, Liu G, Wu J, Yang J and Dong S 2017 Enhanced Resonance
31 Magnetoelectric Coupling in (1-1) Connectivity Composites *Adv. Mater.* **29** n/a-n/a
32
33 [25] Bichurin M I, Filippov D A, Petrov V M, Laletsin V M, Paddubnaya N and Srinivasan
34 G 2003 Resonance magnetoelectric effects in layered magnetostrictive-piezoelectric
35 composites *Phys. Rev. B* **68** 132408
36
37 [26] Gheevarghese V, Laletsin U, Petrov V M, Srinivasan G and Fedotov N A 2007 Low-
38 frequency and resonance magnetoelectric effects in lead zirconate titanate and single-
39 crystal nickel zinc ferrite bilayers *J. Mater. Res.* **22** 2130–5
40
41 [27] Venkata Ramanaa M, Ramamanohar Reddy N, Sreenivasulu G, Siva kumar K V,
42 Murty B S and Murthy V R K 2009 Enhanced magnetoelectric voltage in multiferroic
43 particulate Ni_{0.83}Co_{0.15}Cu_{0.02}Fe_{1.90}O_{4-δ}/PbZr_{0.52}Ti_{0.48}O₃ composites – dielectric,
44 piezoelectric and magnetic properties *Curr. Appl. Phys.* **9** 1134–9
45
46 [28] Leung C M, Zhuang X, Friedrichs D, Li J, Erickson R W, Laletin V, Popov M,
47 Srinivasan G and Viehland D 2017 Highly efficient solid state magnetoelectric gyrators
48 *Appl. Phys. Lett.* **111** 122904
49
50 [29] Cho K-H, Yan Y, Folgar C and Priya S 2014 Zigzag-shaped piezoelectric based high
51 performance magnetoelectric laminate composite *Appl. Phys. Lett.* **104** 222901
52
53
54
55
56
57
58
59
60

- 1
2
3 [30] Wang Y, Gao J, Li M, Hasanyan D, Shen Y, Li J, Viehland D and Luo H 2012
4 Ultralow equivalent magnetic noise in a magnetoelectric Metglas/Mn-doped
5 $\text{Pb}(\text{Mg}_{1/3}\text{Nb}_{2/3})\text{O}_3\text{-PbTiO}_3$ heterostructure *Appl. Phys. Lett.* **101** 022903
6
7 [31] Sreenivasulu G, Petrov V M, Fetisov L Y, Fetisov Y K and Srinivasan G 2012
8 Magnetolectric interactions in layered composites of piezoelectric quartz and
9 magnetostrictive alloys *Phys. Rev. B* **86** 214405
10
11 [32] Sreenivasulu G, Fetisov L Y, Fetisov Y K and Srinivasan G 2012 Piezoelectric single
12 crystal langatate and ferromagnetic composites: Studies on low-frequency and
13 resonance magnetolectric effects *Appl. Phys. Lett.* **100** 052901
14
15 [33] Jin J, Lu S-G, Chanthad C, Zhang Q, Haque M A and Wang Q 2011 Multiferroic
16 Polymer Composites with Greatly Enhanced Magnetolectric Effect under a Low
17 Magnetic Bias *Adv. Mater.* **23** 3853–8
18
19 [34] Freeman E, Harper J, Goel N, Gilbert I, Unguris J, Schiff S J and Tadigadapa S 2017
20 Improving the magnetolectric performance of Metglas/PZT laminates by annealing in
21 a magnetic field *Smart Mater. Struct.* **26** 085038
22
23 [35] Xin C, Ma J, Ma J and Nan C 2017 Stretch-shear mode laminated metglas/Pb (Zr, Ti)
24 O-3/metglas composite with an enhanced magnetolectric effect *Sci. Bull.* **6** 004
25
26 [36] Zeng L, Zhou M, Bi K and Lei M 2016 Giant magnetolectric effect in negative
27 magnetostrictive/piezoelectric/positive magnetostrictive semiring structure *J. Appl.*
28 *Phys.* **119** 034102
29
30 [37] Zhang J, Kang Y, Yu Y and Gao Y 2017 Enhancement of the magnetolectric
31 coupling in an A-line shape magnetostrictive/piezoelectric structure *Phys. Lett. A* **381**
32 1–9
33
34 [38] Hu J-M, Li Z, Wang J and Nan C W 2010 Electric-field control of strain-mediated
35 magnetolectric random access memory *J. Appl. Phys.* **107** 093912
36
37 [39] Hu J-M, Li Z, Wang J, Ma J, Lin Y H and Nan C W 2010 A simple bilayered
38 magnetolectric random access memory cell based on electric-field controllable domain
39 structure *J. Appl. Phys.* **108** 043909
40
41 [40] Tellegen B D 1948 The gyrator, a new electric network element *Philips Res Rep* **3** 81–
42 101
43
44 [41] Zhai J, Li J, Dong S, Viehland D and Bichurin M I 2006 A quasi(unidirectional)
45 Tellegen gyrator *J. Appl. Phys.* **100** 124509
46
47 [42] Gao J, Gray D, Shen Y, Li J and Viehland D 2011 Enhanced dc magnetic field
48 sensitivity by improved flux concentration in magnetolectric laminates *Appl. Phys.*
49 *Lett.* **99** 153502
50
51 [43] Shen L, Li M, Gao J, Shen Y, Li J F, Viehland D, Zhuang X, Lam Chok Sing M,
52 Cordier C, Saez S and Dolabdjian C 2011 Magnetolectric nonlinearity in
53 magnetolectric laminate sensors *J. Appl. Phys.* **110** 114510
54
55
56
57
58
59
60

- 1
2
3 [44] Li M, Wang Z, Wang Y, Li J and Viehland D 2013 Giant magnetoelectric effect in
4 self-biased laminates under zero magnetic field *Appl. Phys. Lett.* **102** 082404
5
6 [45] Zhuang X, Sing M L C, Cordier C, Saez S, Dolabdjian C, Das J, Gao J, Li J and
7 Viehland D 2011 Analysis of Noise in Magnetoelectric Thin-Layer Composites Used
8 as Magnetic Sensors *IEEE Sens. J.* **11** 2183–8
9
10 [46] Kiser J, Lacombe R, Bussmann K, Hawley C J, Spanier J E, Zhuang X, Dolabdjian C,
11 Lofland S and Finkel P 2014 Magnetostrictive stress reconfigurable thin film resonators
12 for near direct current magnetoelectric sensors *Appl. Phys. Lett.* **104** 072408
13
14 [47] Nan T, Hui Y, Rinaldi M and Sun N X 2013 Self-Biased 215MHz Magnetoelectric
15 NEMS Resonator for Ultra-Sensitive DC Magnetic Field Detection *Sci. Rep.* **3** 1985
16
17 [48] Fetisov Y K, Serov V N, Fetisov L Y, Makovkin S A, Viehland D and Srinivasan G
18 2016 A magnetoelectric composite based signal generator *Appl. Phys. Lett.* **108** 213502
19
20 [49] Coblenz W S and Wartenberg S A 2012 The DARPA HUMS program: revolutionizing
21 magnetic field sensors using multiferroic materials and atomic gas vapor cells
22 Unattended Ground, Sea, and Air Sensor Technologies and Applications XIV vol 8388
23 (International Society for Optics and Photonics) p 838809
24
25 [50] Xing Z, Dong S, Zhai J, Yan L, Li J and Viehland D 2006 Resonant bending mode of
26 Terfenol-D/steel/Pb(Zr,Ti)O₃ magnetoelectric laminate composites *Appl. Phys. Lett.* **89**
27 112911
28
29 [51] Dong S, Zhai J, Xing Z, Li J and Viehland D 2007 Giant magnetoelectric effect (under
30 a dc magnetic bias of 2Oe) in laminate composites of FeBSiC alloy ribbons and
31 Pb(Zn_{1/3},Nb_{2/3})O₃–7%PbTiO₃ fibers *Appl. Phys. Lett.* **91** 022915
32
33 [52] Annapureddy V, Palneedi H, Yoon W-H, Park D-S, Choi J-J, Hahn B-D, Ahn C-W,
34 Kim J-W, Jeong D-Y and Ryu J 2017 A pT/ $\sqrt{\text{Hz}}$ sensitivity ac magnetic field sensor
35 based on magnetoelectric composites using low-loss piezoelectric single crystals *Sens.*
36 *Actuators Phys.* **260** 206–11
37
38 [53] Zhuang X, Cordier C, Saez S, Lam Chok Sing M, Dolabdjian C, Gao J, Li J F and
39 Viehland D 2011 Theoretical analysis of the intrinsic magnetic noise spectral density of
40 magnetostrictive-piezoelectric laminated composites *J. Appl. Phys.* **109** 124512
41
42 [54] Gao J, Wang Z, Shen Y, Li M, Wang Y, Finkel P, Li J and Viehland D 2012 Self-
43 powered low noise magnetic sensor *Mater. Lett.* **82** 178–80
44
45 [55] Bhaskaran H, Li M, Garcia-Sanchez D, Zhao P, Takeuchi I and Tang H X 2011 Active
46 microcantilevers based on piezoresistive ferromagnetic thin films *Appl. Phys. Lett.* **98**
47 013502
48
49 [56] Zhuang X, Sing M L C, Dolabdjian C, Wang Y, Finkel P, Li J and Viehland D 2015
50 Mechanical Noise Limit of a Strain-Coupled Magneto(Elasto)electric Sensor Operating
51 Under a Magnetic or an Electric Field Modulation *IEEE Sens. J.* **15** 1575–87
52
53
54
55
56
57
58
59
60

- 1
2
3 [57] Mandal S K, Sreenivasulu G, Petrov V M and Srinivasan G 2010 Flexural deformation
4 in a compositionally stepped ferrite and magnetoelectric effects in a composite with
5 piezoelectrics *Appl. Phys. Lett.* **96** 192502
6
7 [58] Zhuang X, Saez S, Lam Chok Sing M, Cordier C, Dolabdjian C, Li J, Viehland D,
8 Mandal S K, Sreenivasulu G and Srinivasan G 2012 Investigation on the Magnetic
9 Noise of Stacked Magnetostrictive-Piezoelectric Laminated Composites *Sens. Lett.* **10**
10 961–5
11
12 [59] Chen Y, Gillette S M, Fitchorov T, Jiang L, Hao H, Li J, Gao X, Geiler A, Vittoria C
13 and Harris V G 2011 Quasi-one-dimensional miniature multiferroic magnetic field
14 sensor with high sensitivity at zero bias field *Appl. Phys. Lett.* **99** 042505
15
16 [60] Srinivasan G, Rasmussen E T, Gallegos J, Srinivasan R, Bokhan Y I and Laletin V M
17 2001 Magnetoelectric bilayer and multilayer structures of magnetostrictive and
18 piezoelectric oxides *Phys. Rev. B* **64** 214408
19
20 [61] Li M, Berry D, Das J, Gray D, Li J and Viehland D 2011 Enhanced Sensitivity and
21 Reduced Noise Floor in Magnetoelectric Laminate Sensors by an Improved Lamination
22 Process *J. Am. Ceram. Soc.* **94** 3738–41
23
24 [62] Wang Y, Gray D, Berry D, Li M, Gao J, Li J and Viehland D 2012 Influence of
25 interfacial bonding condition on magnetoelectric properties in piezofiber/Metglas
26 heterostructures *J. Alloys Compd.* **513** 242–4
27
28 [63] Filippov D A, Galichyan T A and Laletin V M 2014 Influence of an interlayer bonding
29 on the magnetoelectric effect in the layered magnetostrictive-piezoelectric structure
30 *Appl. Phys. A* **116** 2167–71
31
32 [64] Quandt E, Stein S and Wuttig M 2005 Magnetic vector field sensor using
33 magnetoelectric thin-film composites *IEEE Trans. Magn.* **41** 3667–9
34
35 [65] Piorra A, Jahns R, Teliban I, Gugat J L, Gerken M, Knöchel R and Quandt E 2013
36 Magnetoelectric thin film composites with interdigital electrodes *Appl. Phys. Lett.* **103**
37 032902
38
39 [66] Rübisch V, Salzer S, Urs N O, Reermann J, Yarar E, Piorra A, Kirchhof C, Lage E,
40 Höft M, Schmidt G U, Knöchel R, McCord J, Quandt E and Meyners D 2017 Pushing
41 the detection limit of thin film magnetoelectric heterostructures *J. Mater. Res.* **32** 1009–
42 19
43
44 [67] Yarar E, Salzer S, Hrkac V, Piorra A, Höft M, Knöchel R, Kienle L,
45 and Quandt E 2016 Inverse bilayer magnetoelectric thin film sensor *Appl. Phys. Lett.*
46 **109** 022901
47
48 [68] Xing Z, Zhai J, Li J and Viehland D 2009 Investigation of external noise and its
49 rejection in magnetoelectric sensor design *J. Appl. Phys.* **106** 024512
50
51 [69] Salzer S, Durdaut P, Rübisch V, Meyners D, Quandt E, Höft M and Knöchel R 2017
52 Generalized Magnetic Frequency Conversion for Thin-Film Laminate Magnetoelectric
53 Sensors *IEEE Sens. J.* **17** 1373–83
54
55
56
57
58
59
60

- 1
2
3 [70] Xu J, Zhuang X, Leung C, Staruch M., Finkel P, Li J and Viehland D 2018
4 Magnetolectric gradiometer with enhanced vibration rejection efficiency under H-
5 field modulation *J. Appl. Phys.* **123** 104501
6
7 [71] Zhang J, Li P, Wen Y, He W, Yang J, Yang A, Lu C and Li W 2014 Enhanced
8 sensitivity in magnetolectric current-sensing devices with frequency up-conversion
9 mechanism by modulating the magnetostrictive strain *J. Appl. Phys.* **115** 17E505
10
11 [72] Shen Y, Gao J, Wang Y, Li J and Viehland D 2014 High non-linear magnetolectric
12 coefficient in Metglas/PMN-PT laminate composites under zero direct current magnetic
13 bias *J. Appl. Phys.* **115** 094102
14
15 [73] Shen Y, Gao J, Wang Y, Finkel P, Li J and Viehland D 2013 Piezomagnetic strain-
16 dependent non-linear magnetolectric response enhancement by flux concentration
17 effect *Appl. Phys. Lett.* **102** 172904
18
19 [74] Wang Y, Shen Y, Gao J, Li M, Li J and Viehland D 2013 Nonlinear magnetolectric
20 response of a Metglas/piezofiber laminate to a high-frequency bipolar AC magnetic
21 field *Appl. Phys. Lett.* **102** 102905
22
23 [75] Wang Y, Finkel P, Li J and Viehland D 2014 Piezoelectric single crystal and
24 magnetostrictive Metglas composites: Linear and nonlinear magnetolectric coupling
25 *Appl. Phys. Lett.* **104** 142909
26
27 [76] Li M, Wang Y, Shen Y, Gao J, Li J and Viehland D 2013 Structural dependence of
28 nonlinear magnetolectric effect for magnetic field detection by frequency modulation
29 *J. Appl. Phys.* **114** 144501
30
31 [77] Huang J, O'Handley R C and Bono D 2003 New high-sensitivity hybrid
32 magnetostrictive/electroactive magnetic field sensors *Smart Structures and Materials*
33 *2003: Smart Sensor Technology and Measurement Systems vol 5050 (International*
34 *Society for Optics and Photonics)* pp 229–38
35
36 [78] Dai X, Wen Y, Li P, Yang J and Zhang G 2009 Modeling, characterization and
37 fabrication of vibration energy harvester using Terfenol-D/PZT/Terfenol-D composite
38 transducer *Sens. Actuators Phys.* **156** 350–8
39
40 [79] Dai X, Wen Y, Li P, Yang J and Li M 2011 Energy harvesting from mechanical
41 vibrations using multiple magnetostrictive/piezoelectric composite transducers *Sens.*
42 *Actuators Phys.* **166** 94–101
43
44 [80] Yang J, Wen Y, Li P and Bai X 2011 A magnetolectric-based broadband vibration
45 energy harvester for powering wireless sensors *Sci. China Technol. Sci.* **54** 1419–27
46
47 [81] Bai X, Wen Y, Li P, Yang J, Peng X and Yue X 2014 Multi-modal vibration energy
48 harvesting utilizing spiral cantilever with magnetic coupling *Sens. Actuators Phys.* **209**
49 78–86
50
51 [82] Lin Z, Yang J, Zhao J, Zhao N, Liu J, Wen Y and Li P 2016 Enhanced Broadband
52 Vibration Energy Harvesting Using a Multimodal Nonlinear Magnetolectric Converter
53 *J. Electron. Mater.* **45** 3554–61
54
55
56
57
58
59
60

- 1
2
3 [83] Yang J, Wen Y, Li P, Yue X and Bai X 2012 A bi-axial and wideband vibration
4 energy harvester using magnetoelectric transducer *2012 IEEE International*
5 *Ultrasonics Symposium 2012 IEEE International Ultrasonics Symposium* pp 2404–7
6
7 [84] Moss S D, McLeod J E, Powlesland I G and Galea S C 2012 A bi-axial
8 magnetoelectric vibration energy harvester *Sens. Actuators Phys.* **175** 165–8
9
10 [85] Lin Z, Chen J, Li X, Li J, Liu J, Awais Q and Yang J 2016 Broadband and three-
11 dimensional vibration energy harvesting by a non-linear magnetoelectric generator
12 *Appl. Phys. Lett.* **109** 253903
13
14 [86] Zhu Y and Zu J W 2012 A Magnetoelectric Generator for Energy Harvesting From the
15 Vibration of Magnetic Levitation *IEEE Trans. Magn.* **48** 3344–7
16
17 [87] Li M, Wen Y, Li P and Yang J 2013 A resonant frequency self-tunable rotation energy
18 harvester based on magnetoelectric transducer *Sens. Actuators Phys.* **194** 16–24
19
20 [88] Dai X 2016 An vibration energy harvester with broadband and frequency-doubling
21 characteristics based on rotary pendulums *Sens. Actuators Phys.* **241** 161–8
22
23 [89] Bayrashev A, Robbins W P and Ziaie B 2004 Low frequency wireless powering of
24 microsystems using piezoelectric–magnetostrictive laminate composites *Sens.*
25 *Actuators Phys.* **114** 244–9
26
27 [90] Wang Y, Zhao X, Jiao J, Liu L, Di W, Luo H and Or S W 2010 Electrical resistance
28 load effect on magnetoelectric coupling of magnetostrictive/piezoelectric laminated
29 composite *J. Alloys Compd.* **500** 224–6
30
31 [91] Gao J, Hasanyan D, Shen Y, Wang Y, Li J and Viehland D 2012 Giant resonant
32 magnetoelectric effect in bi-layered Metglas/Pb(Zr,Ti)O₃ composites *J. Appl. Phys.*
33 **112** 104101
34
35 [92] Qiu J, Wen Y, Li P and Yang J 2012 Design and testing of piezoelectric energy
36 harvester for powering wireless sensors of electric line monitoring system *J. Appl.*
37 *Phys.* **111** 07E510
38
39 [93] He W, Li P, Wen Y, Zhang J, Yang A and Lu C 2014 A Noncontact Magnetoelectric
40 Generator for Energy Harvesting From Power Lines *IEEE Trans. Magn.* **50** 1–4
41
42 [94] Leland E S, White R M and Wright P K 2006 Energy scavenging power sources for
43 household electrical monitoring *Proc. PowerMEMS* vol 77
44
45 [95] He W, Li P, Wen Y, Zhang J, Yang A and Lu C 2014 Energy Harvesting From Two-
46 Wire Power Cords Using Magnetoelectric Transduction *IEEE Trans. Magn.* **50** 1–5
47
48 [96] Dong S, Zhai J, Li J F, Viehland D and Priya S 2008 Multimodal system for harvesting
49 magnetic and mechanical energy *Appl. Phys. Lett.* **93** 103511
50
51 [97] Lasheras A, Gutiérrez J, Reis S, Sousa D, Silva M, Martins P, Lanceros-Mendez S,
52 Barandiarán J M, Shishkin D A and Potapov A P 2015 Energy harvesting device based
53 on a metallic glass/PVDF magnetoelectric laminated composite *Smart Mater. Struct.* **24**
54 065024
55
56
57
58
59
60

- 1
2
3 [98] Zhou Y, Apo D J and Priya S 2013 Dual-phase self-biased magnetoelectric energy
4 harvester *Appl. Phys. Lett.* **103** 192909
5
6 [99] Qiu J, Wen Y, Li P and Chen H 2015 Design and Optimization of a Tunable
7 Magnetoelectric and Electromagnetic Hybrid Vibration-Based Generator for Wireless
8 Sensor Networks *IEEE Trans. Magn.* **51** 1–4
9
10 [100] Dong S, Li J F and Viehland D 2004 Voltage gain effect in a ring-type magnetoelectric
11 laminate *Appl. Phys. Lett.* **84** 4188–90
12
13 [101] Dong S, Li J F, Viehland D, Cheng J and Cross L E 2004 A strong magnetoelectric
14 voltage gain effect in magnetostrictive-piezoelectric composite *Appl. Phys. Lett.* **85**
15 3534–6
16
17 [102] Wang Y, Zhao X, Di W, Luo H and Or S W 2009 Magnetoelectric voltage gain effect
18 in a long-type magnetostrictive/piezoelectric heterostructure *Appl. Phys. Lett.* **95**
19 143503
20
21 [103] Lü L, Guo Y, Zhou J, Wang P, Liu P and Chen X 2011 Adjusting the voltage step-up
22 ratio of a magnetoelectric composite transformer *Chin. Sci. Bull.* **56** 700–3
23
24 [104] Zhou Y, Yan Y and Priya S 2014 Co-fired magnetoelectric transformer *Appl. Phys.*
25 *Lett.* **104** 232906
26
27 [105] Zhai J, Gao J, Vreugd C D, Li J, Viehland D, Filippov A V, Bichurin M I, Drozdov D
28 V, Semenov G A and Dong S X 2009 Magnetoelectric gyrator *Eur. Phys. J. B* **71** 383
29
30 [106] Zhuang X, Leung C M, Li J and Viehland D 2017 Evaluation of magnetomechanical
31 conversion efficiencies in magnetoelectric gyrators *AIP Adv.* **8** 056607
32
33 [107] Leung C M, Zhuang X, Xu J, Srinivasan G, Li J and Viehland D 2016 Power
34 conversion efficiency and resistance tunability in coil-magnetoelectric gyrators *Appl.*
35 *Phys. Lett.* **109** 202907
36
37 [108] Dong S, Li J-F and Viehland D 2006 Magnetoelectric coupling, efficiency, and voltage
38 gain effect in piezoelectric-piezomagnetic laminate composites *Frontiers of*
39 *Ferroelectricity* (Springer, Boston, MA) pp 97–106
40
41 [109] Zhuang X VT Internal report No 5
42
43 [110] Leung C M, Zhuang X, Xu J, Li J, Srinivasan G and Viehland D 2017 Importance of
44 composite parameters in enhanced power conversion efficiency of Terfenol-D/PZT
45 magnetoelectric gyrators *Appl. Phys. Lett.* **110** 112904
46
47 [111] Zhuang X, Leung C M, Li J and Viehland D 2017 Power conversion process in
48 magnetoelectric gyrators *Appl. Phys. Lett.* **111** 103902
49
50 [112] Leung C M, Zhuang X, Gao M, Tang X, Xu J, Li J, Zhang J, Srinivasan G and
51 Viehland D 2017 Enhanced stability of magnetoelectric gyrators under high power
52 conditions *Appl. Phys. Lett.* **111** 182901
53
54
55
56
57
58
59
60

- 1
2
3 [113] Zhuang X, Leung C M, Sreenivasulu G, Gao M, Zhang J, Srinivasan G, Li J and
4 Viehland D 2017 Upper limit for power conversion in magnetoelectric gyrators *Appl.*
5 *Phys. Lett.* **111** 163902
6
7 [114] NASA, Mars inSight Mission. www.nasa.gov
8
9 [115] Department of Energy, What the smart grid means to America's future.
10 www.smartgrid.gov
11
12 [116] T. Ohira, 2017 A battery-less electric roadway vehicle runs for the first time in the
13 world Proc. IEEE Int. Conf. Microwaves Intelligent Mobility, Nagoya
14
15 [117] Departement of Defense, A MEchanically Based Antenna, <https://www.darpa.mil>
16
17
18
19
20
21
22
23
24
25
26
27
28
29
30
31
32
33
34
35
36
37
38
39
40
41
42
43
44
45
46
47
48
49
50
51
52
53
54
55
56
57
58
59
60